Coordination Chemistry Reviews 284 (2015) 1–18

Contents lists available at ScienceDirect

Coordination Chemistry Reviews

journal homepage: www.elsevier.com/locate/ccr

Review

Applications of chiroptical spectroscopy to coordination compounds

Tao Wu [a,b,*], Xiao-Zeng You [a], Petr Bouř [b]

[a] State Key Laboratory of Coordination Chemistry, School of Chemistry and Chemical Engineering, Nanjing National Laboratory of Microstructures, Nanjing University, 210093 Nanjing, PR China
[b] Institute of Organic Chemistry and Biochemistry, Academy of Sciences, Flemingovo nám. 2, 16610 Prague, Czech Republic

Contents

ARTICLE INFO

Article history:
Received 16 June 2014
Accepted 19 September 2014
Available online 28 September 2014

Keywords:
Chirality
Coordination compounds
Chiroptical spectroscopy
New materials

ABSTRACT

Chiroptical methods represent indispensable tools for structural studies of chiral coordination compounds. Numerous applications in asymmetric catalysis, chiral recognition, chiral materials, and supramolecules stabilized by metals have fuelled their ongoing development. Materials derived from chiral coordination compounds have attracted considerable interest due to the possibility to fine-tune their physical properties through versatile chemical synthesis. This review provides an overview of the applicability range of chiroptical methods as a principle tool for chirality investigation, and typical applications of chiral coordination chemistry. The potential of electronic and vibrational chiroptical methods in the design and characterization of coordination compounds is discussed. The electronic optical activity in the form of circular dichroism (CD) continues to be the most frequent tool in stereo-chemical analysis. The potential of vibrational optical activity (VOA) for chiral coordination compounds is still poorly explored, especially when compared with VOA's role in organic chemistry and biochemistry. However, the vibrational region can often provide unique and more detailed information than the electronic methods, because of higher spectroscopic resolution, reduced dependence on characteristic chromophores, and better reproducibility of the spectra by theoretical methods.

1. Introduction

Chirality, the so called left- and right-hand symmetry, is defined in chemistry by IUPAC as: The geometric property of a rigid object (or spatial arrangement of points or atoms) of being nonsuperimposable on its mirror image; such an object has no symmetry elements of the second kind (a mirror plane, $\sigma = S_1$, a centre of inversion, $i = S_2$, a rotation reflection axis, S_{2n}). If the object is

* Corresponding author. Tel.: +420 220183 445.
E-mail addresses: njutwu@gmail.com (T. Wu), youxz@nju.edu.cn (X.-Z. You), bour@uochb.cas.cz (P. Bouř).

http://dx.doi.org/10.1016/j.ccr.2014.09.012
0010-8545/

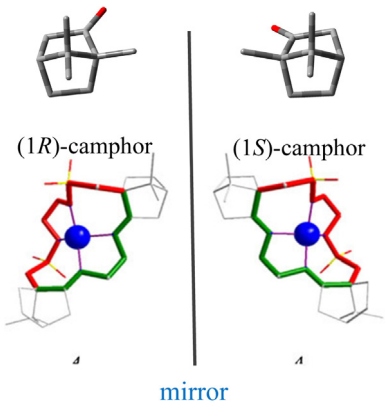

Fig. 1. Examples of chirality of an organic compound, camphor (top), and a copper(II) coordination compound (containing the camphor residue, too, bottom).

superimposable on its mirror image the object is described as being achiral [1]. Molecular chirality is essential for the functioning of living organisms. For coordination compounds, the issue of chirality emerged almost as early as the coordination chemistry was founded by Alfred Werner [2]. Chirally resolved (enantiomeric) coordination compounds could be utilized in many domains of chemistry including asymmetric catalysis, chiral recognition, chiral materials, and supramolecular chemistry [3].

In spite of that, chirality is not so frequently explored in coordination chemistry as it is in organic chemistry and biochemistry [4]. One of the reasons may be the complicated relation between the geometry and electronic configuration of coordination compounds. Heavy metals contain d and higher angular-momentum orbitals, sometimes spin-polarized, and the theoretical description is more complicated than for the majority of organic compounds, often containing s and p orbitals only. Additionally, for elements of higher atomic number, relativistic effects cannot be neglected [5].

In metal complexes, chirality is often realized by an asymmetric ligand arrangement around one or several coordination centres of high coordination number [2,6]. To some extent, the metal plays the role of the asymmetric carbon in organic molecules, often with a similar chiral scaffold (Fig. 1). The chiral arrangement is variable in crystals in which optically active compounds (both organic and inorganic) may belong to one of 15 symmetry point groups, C_1, C_s, C_2, C_{2v}, D_{2v}, C_3, D_3, C_4, S_4, D_{2d}, D_4, C_6, D_6, T, and O.

The most common coordination compounds that are chiral at molecular level possess elements of octahedral (OC-6), tetrahedral (T-4), distorted square planar (SP-4), and helical symmetries. According to the milestone work of Zelewsky, the transfer of chirality from ligand to the metal ion centre is the most efficient way of asymmetric synthesis of coordination compounds [7].

A remarkably large variety of coordination compounds has been prepared via a self-assembly of metal ions and optically active ligands. Their properties are relatively well-predictable from geometry and cooperative effects [3,8].

Materials made from coordination compounds have thus been attracting attention as their physical properties may be fine-tuned through versatile chemical synthesis [9]. Materials exhibiting multiple optical, electrical, and magnetic properties are sometimes referred to as multi-functional [10].

Optical spectroscopic methods can be conveniently utilized to study the synergetic effects between the geometry and physical properties due to manipulated chirality. Chiroptical spectroscopies are based on the interaction of chiral matter with left- and right-circularly polarized light [11].

Historically, optical rotation and the optical rotation dispersion (ORD) were the easiest methods to apply. However, the spectra were difficult to interpret in terms of the structure, as the rotation at each wavelength comprises contributions of many electronic transitions. Currently, the most widely applied technique is thus *circular dichroism* (CD) detecting the absorption difference between left- and right-circularly polarized light for individual transitions (Fig. 2). It includes the traditional electronic CD (ECD) sensing electronic transitions and sometimes referred to as ultra-violet CD (UVCD), although commercially available spectrometers cover a broad range of wavelengths (~180–800 nm). This range may be severely restricted by the solvent transmission, material of the sample cell, etc. Below 180 nm, special vacuum techniques and synchrotron radiation can be used as the source of light. Low-lying electronic transitions, for example in lanthanide complexes, can be seen by extending the wavelength range to the near-infrared region (800–1100 nm).

Theoretically, a technique akin to ECD is circularly polarized luminescence (CPL). It detects transitions from the excited states, i.e. it measures the differences in emission of the left- and right-circularly polarized light [12].

In 1970s, molecular vibrational optical activity (VOA) was developed [13], which brought about the possibility to study the vibrational transitions, usually more numerous and better resolved than the electronic ones. Additionally, the calculation of VOA spectra is easier than for the electronic ones since one only needs to model the electronic ground state.

The instrumentation for vibrational analogue of ECD, vibrational circular dichroism (VCD), has been commercially available since about 1997. The technique operates with infrared radiation.

Somewhat less common is the other form of VOA, Raman optical activity (ROA) which detects the differences in scattering intensities of right- and left-circularly polarized light. ROA instrumentation has been commercially available since about 2003.

Table 1 summarizes some basic properties of various chiroptical techniques. However, any categorical division is only approximate. For example, VOA spectroscopies can also include contributions from low-lying electronic states; VCD has also been extended to the near-infrared region (NIR-VCD), although applications in coordination chemistry have not been reported so far [14].

Unlike for simple infrared absorption, VCD optical elements limit the wavenumber range and sometimes the choice of solvent. Also, samples suitable for VCD measurement should exhibit absorbance in a relatively narrow range of 0.1–1.0; the most desirable value is ca. 0.5. The absorbance can be optimized by a combination of sample concentration, optical pathlength, and the choice of solvent. Deuterated organic solvents are frequently employed in order to reduce the absorbance and broaden the spectroscopic window. For insoluble compounds, solid state VCD may be helpful while employing dispersion in mineral oil, or KBr pellet.

Compared with VCD, ROA measurement requires even slightly higher sample concentration on average. Note that for many compounds the recommended concentrations in Table 1 are not possible due to the limited solubility. Unlike for VCD, water is a very good solvent for the Raman techniques, whereas scattering from organic solvents often masks the signal from the sample. Although theoretically possible [15], ROA above ~2400 cm^{-1} is rarely measured due to the limits of the coupled-charge detector. Both of the VOA methods (VCD and ROA) are more reliable than the electronic ones to determine the conformation or absolute configuration.

ORD and ECD are probably the most flexible and most sensitive techniques. Many organic solvents enabling ECD measurement in a large part of the 180–800 nm intervals are available, and the concentration can be lower than for VOA. The electronic spectra, however, provide a limited number of features, not necessarily associated with local geometry. ECD interpretation requires rather extensive computations of excited electronic states, for which available methods provide a limited precision only.

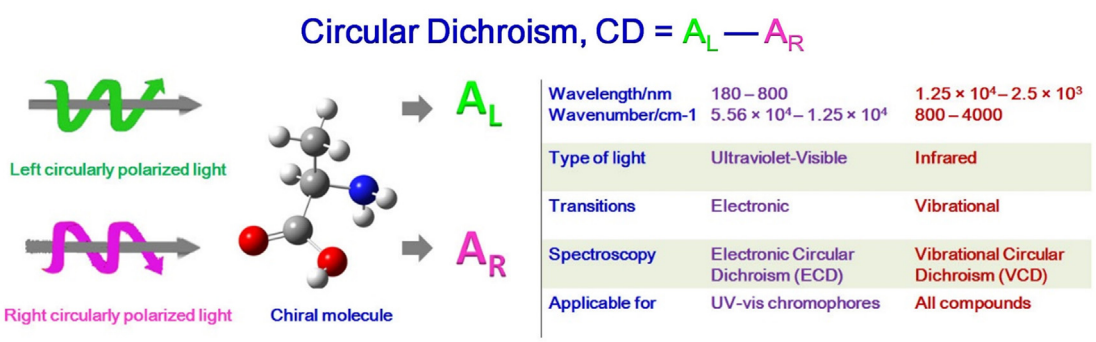

Fig. 2. Schematic description of CD, A_L and A_R are absorptions of left- and right-circularly polarized light.

2. Chiroptical spectroscopic methods in coordination chemistry

2.1. Electronic circular dichroism (ECD) and optical rotatory dispersion (ORD)

Let us recall that absorption and circular dichroism spectra consist of peaks typically characterized by their positions (λ_{max}, $\tilde{\nu}_{max}$), maximal/minimal intensities (ε_{max}, $\Delta\varepsilon_{max}$, $\Delta\varepsilon_{min}$), and bandwidths. The sign of a CD band represents the principal advantage against the absorption as it brings about enhanced structural information. All systems studied by ECD are also amenable to ORD; however, the latter technique monitors a combined contribution of all electronic states, and is used less frequently for structural determination.

For studying CD, studied compounds must absorb in the accessible range of wavelengths (Fig. 2). Very frequently, charge-transfer (CT) excited states in coordination compounds enable ECD measurement useful for absolute configuration determination [16].

Determination of molecular structure is dependent on a good theoretical model. Reliable computations of molecular excited states are confined to small systems. ECD and ORD spectra of larger molecules can usually be predicted with a good accuracy using the time-dependent density functional theory (TDDFT) [17]. Yet accurate TDDFT predictions of ECD spectra of transition metal complexes are very difficult. The calculated spectra are strongly dependent on the functional employed since most functionals were optimized for light elements. The ECD signal of the d–d transitions is often very weak and beyond the computational accuracy. Often, convergence problems are encountered, especially for open shell systems [18].

The first TDDFT predictions of ECD spectra of coordination compounds were reported in 2003 [19]. Afterwards, a number of computations on ECD spectra of transition metal complexes appeared [20]. For example, Ziegler et al. performed theoretical ECD predictions of tris-diamine Co(III) and Rh(III) complexes. They verified that TDDFT was able to capture major differences in the ECD spectra of complexes with the Λ-configuration, and their isomers with the Δ-configuration, both in the d–d and ligand-to-metal CT (LMCT) region [20(a)]. Analysis of other coordination compounds $[M(bpy)_3]^{2+}$ (M = Fe, Ru, Os) provided insight into the ECD origin, caused by d–d and metal-to-ligand CT (MLCT) transitions, analogously to the ligand charge exciton excitations [20(d)]. Wang et al. analyzed three kinds of ruthenium-chelating tris-diamine complexes to quantitatively assess the individual contributions of the Δ/Λ, R/S, and δ/λ steric arrangements to ECD, and suggested simple rules to directly determine the absolute configurations [20(f)].

Obviously, X-ray single crystal diffraction remains the most reliable method for determination of the absolute configuration, also for coordination compounds. However, growing the desired crystal may not be possible. Structure or conformation adopted in the solid state may differ from that in solution or in the gas phase. In such cases the ECD technique combined with TDDFT calculations can be helpful for stereo-chemical analysis [21].

For example, Bernhard et al. asymmetrically synthesized chiral hemicage metal (M = Ru, Zn, Fe) complexes with predetermined configurations at the metal centres with an optically active ligand. Through comparing the calculated UV–vis and ECD spectra with experimental data, the absolute configuration was found (Fig. 3) [21(c)].

We have asymmetrically synthesized macrocyclic copper coordination compounds enantiomers derived from camphor enantiomers as a model for CD complex studies (Fig. 1) [21(d)]. Their absolute configuration was determined by X-ray crystallography. The TDDFT calculations reproduced the UV–vis and ECD spectra quite well, which enabled reliable assignments of the ECD and absorption bands, and the absolute configuration. Frelek et al. used dimolybdenum carboxylates as ECD auxiliary chromophores for the determination of absolute configuration of optically active *vic*-diols, with the support of DFT calculations. The stereo-analysis enabled them to estimate the most probable geometry of the chiral complex formed in solution (Fig. 4) [22]. Recently, Enamullah et al. reported induced chirality-at-metal and diastereoselectivity at Δ/Λ-configured distorted SP-4 copper complexes derived from bidentate enantiopure Schiff base ligands, the TDDFT simulated ECD spectra for diastereomers revealed that ECD spectra of those complexes were strongly influenced by the configuration of the central copper ion [23].

Table 1
Comparison of the chiroptical techniques.

	ORD	ECD	CPL	VCD	ROA
Cost (10^6 USD)	Cheap	0.1	0.3	0.1	0.2
Usual detection range	180–800 nm	180–800 nm	180–800 nm	800–4000 cm^{-1}	100–2400 cm^{-1}
Typical concentration used	0.1 mg/ml	0.1 mg/ml	0.1 mg/ml	10 mg/ml	30 mg/ml
Theoretical prediction (DFT/TDDFT)	Reliable for large rotations	Usually reliable	Difficult	Very reliable	Very reliable
Water as a solvent	OK	OK	OK	Problematic	Ideal
Organic solvents	OK	OK	OK	Acceptable	Problematic
Solid state measurement	Artefacts	Possible	Possible	Possible	Not known
Peak resolution	Limited	Few bands	Few bands	Many transitions	Many transitions

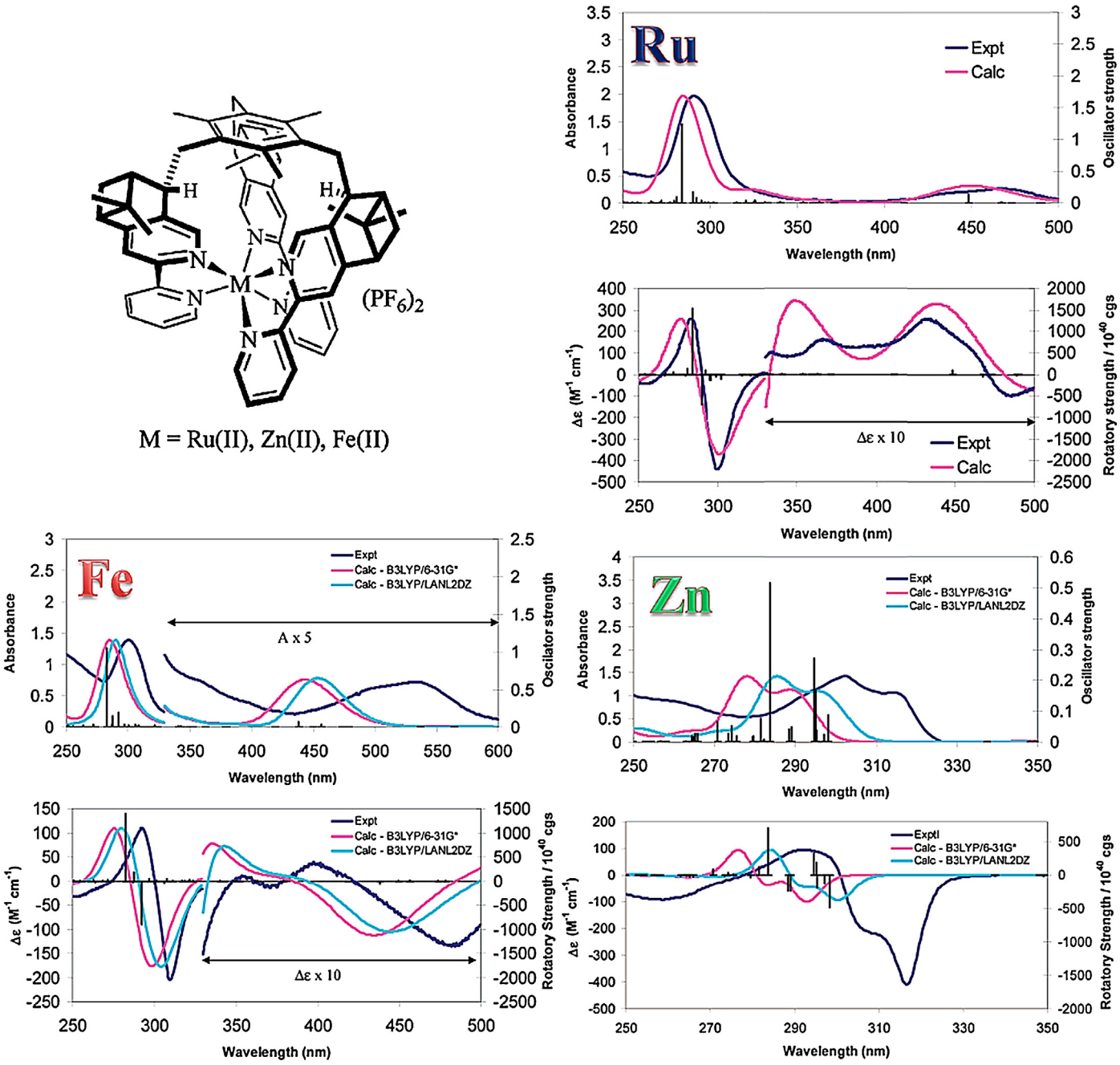

Fig. 3. The structures of chiral hemicage metal complexes and their corresponding experimental and calculated UV–vis and ECD spectra. Reproduced with permission from Ref. [21(c)]. Copyright 2008 American Chemical Society.

The intensities of ECD spectra are particularly strong in compounds and metal complexes that exhibit exciton coupling effects (Fig. 5) [16(a),24], which is sometimes denoted as the exciton-coupled circular dichroism (ECCD). The exciton coupling occurs when two of the same or similar, usually achiral, chromophores are chirally arranged in space. Because of the similarity of the electron energy levels, these are easily perturbed by the interaction. The energy splitting and a large electronic transition dipole moment in each chromophores may lead to a strong ECD signal, often in the form of a couplet, i.e. pair of a positive and negative ECD bands. For example, metallated porphyrin tweezers are widely applied as binding sites in the assignment of absolute configuration of optically active organic compounds based on the ECCD methodology [25]. The optically active guest molecule fixes the exciton-coupled chromophores in space, and thus induces the ECD signal. This usually leads to ECD couplet, also sometimes seen as a combination of positive and negative cotton effects (Fig. 6). Recently, Anslyn and Di Bari presented a new ECCD model by employing a zinc tris(pyridine) complex, interpreted on the basis of TDDFT calculations. The ECD couplet could then be used for stereo-chemical analysis of enantiomeric excess of chiral secondary alcohols (Fig. 7) [26].

Chirality and the excitonic splitting can be utilized to study today very popular molecular switches [27]. Any molecule that can reversibly interconvert between two stable states upon an external stimulus can be considered a molecular switch. Chiroptical switches alter their mode of interaction with circularly polarized light. They serve as key elements in optical displays and other

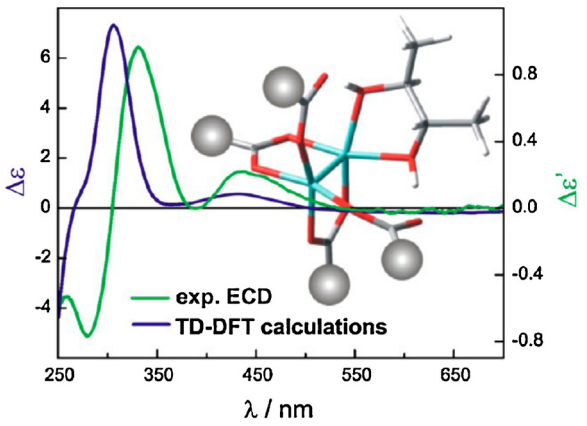

Fig. 4. Structure of dimolybdenum tetracarboxylate chelating *vic*-diol complex involved and their experimental and TDDFT calculated ECD spectra. Reproduced with permission from Ref. [22]. Copyright 2013 American Chemical Society.

materials for molecular electronics. Currently, ECD spectroscopy is most widely applied for the characterization of these materials.

The combination of coordination and redox chemistry can alter conformational states of molecular switches; metal ions then induce structural variances directly. Canary systematically investigated mechanisms useful for the design of chiroptical switches based on coordination compounds [28]. Basic requirements include stability and chemical reversibility of optical active molecules. A high sensitivity of the chiroptical response (such as distinctive ECD signal changes) and multimode switching for potential usage are also necessary. [*n*]Helicenes are good candidates for chirality transfer in coordination chemistry. Crassous et al. reported synthesis of an aza[6]helicene-phosphole as an epimeric mixture of (P,R_P)- and (P,S_P)- conformations with inversion of the configuration at the phosphorus atom (Fig. 8) [29(a)]. Through coordinating with Pd^{II} and Cu^{I} metal ions, Pd^{II} was more efficient than Cu^{I} to promote chiroptical properties (ECD and optical rotations) of these helicene derivatives. The coordination of [*n*]helicenes and transition metals might provide an efficient route to obtain chiroptical switches [29(b)–(d)].

As indicated above, usage of ORD in coordination chemistry is limited, and the theory suffers similar problems as ECD [30].

2.2. Circularly polarized luminescence (CPL)

CPL can be viewed as the emission analogue of ECD, i.e. the light is emitted by an excited state. A strong CPL is typically exhibited by optically active lanthanide complexes [31]. Whereas EDCD (emission-detected circular dichroism or fluorescence-detected circular dichroism FDCD) spectroscopy like conventional CD examines the structure of the ground state, one can say that CPL probes the chirality of the excited state. These spectroscopic examinations are particularly valuable when geometry changes occur during the electronic excitation process; theoretically, with no geometry change and the same states involved in CPL and ECD, the two spectroscopic shapes would be the same. However, CPL modelling often involves energy transfer between molecular energy levels and excited state optimization, quite more complex than for ECD.

Both methods if combined with time resolution bring about information about molecular dynamics and energy changes that occur between the time of the excitation and emission. The combination of ECD and CPL spectra is thus very desirable for analyzing the ground and excited states of transitional metal complexes. Richardson et al. investigated chirality-related structural variances between ground state and ^{3}MLCT emitting states of an osmium(II) polypyridyl complex through comparison of the absorption and emission dissymmetry factors [32]. In the ECD–CPL spectroscopic overlap, the magnitude of observed emission dissymmetry factor was much weaker than the absorption one. The geometry differences between the ground and emitting states were helpful for interpretation of chirality-dependent molecular processes.

Bernhard designed ruthenium(II) and zinc(II) hemicage complexes derived from chiral 2, 2′-bipyridine ligands with controlled

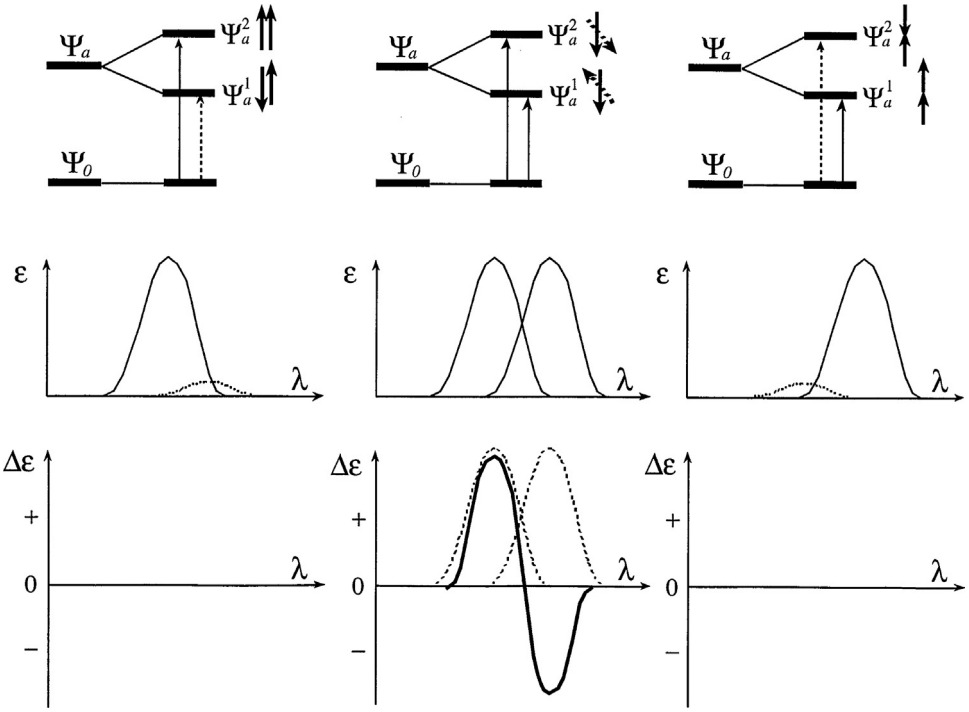

Fig. 5. Exciton coupling of two degenerate transitions, the absorption and ECD spectra: ground states (Ψ_0), excited states (Ψ_a, split into $\Psi_a{}^1$ and $\Psi_a{}^2$ due to the interaction) [16(a)]. Reproduced with a permission of Elsevier.

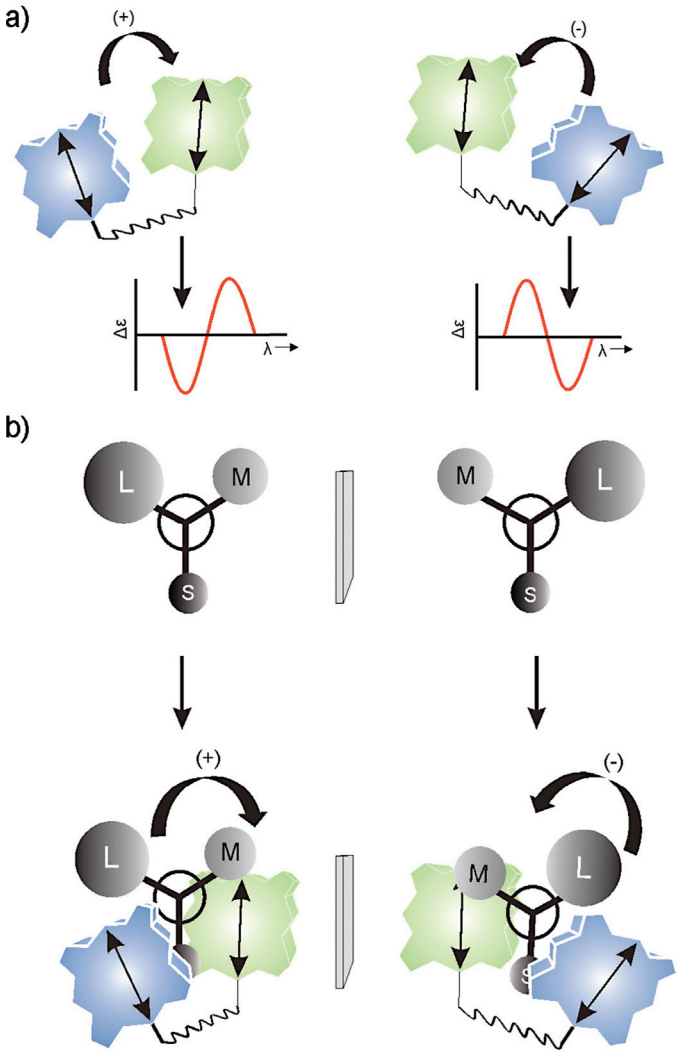

Fig. 6. Induced exciton coupling (a) ECD spectrum is dependent on the porphyrin geometry; the double headed black arrows represent the direction of the transition dipole moment. (b) The chiral orientation is caused, for example, by steric effects; L, M and S mean large, medium and small sized groups in a chiral substrate [25(b)]. Reproduced with a permission of Elsevier.

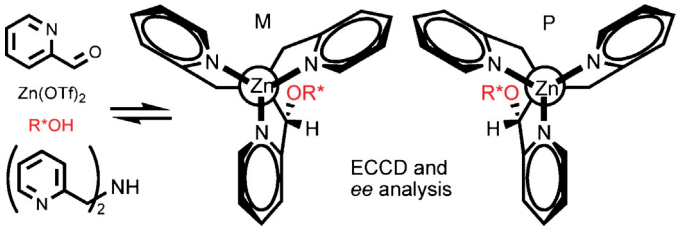

Fig. 7. Zinc(II) tris(pyridine) complex model for ECCD. Reproduced with permission from Ref. [26]. Copyright 2012 American Chemical Society.

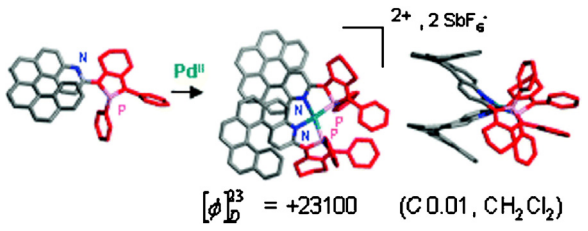

Fig. 8. Stereoselective coordination process of the aza[6]helicenephosphole *P,N*-chelate ligand to Pd^{II} ion. Reproduced with permission from Ref. [29(a)]. Copyright 2009 American Chemical Society.

helicity. Their absolute configuration was verified by ECD and CPL spectroscopies (Fig. 9) [33]. For the zinc complexes, an intersystem crossing occurred during the cage coordination process, leading to a phosphorescent emission of the blue light. Both Zelewsky and Bernhard confirmed that optically active iridium(III) complexes were good candidates for observing CPL [34], in particular the maximum *g* (ratio of CPL and total emission) value for one of the enantiopure compounds reached 2×10^{-3} (Fig. 10) [34(b)]. Bernhard employed TDDFT computations, firstly of the ECD spectra of these iridium(III) complexes, and then extended the calculations to simulate emission dissymmetry, with the aim of establishing reliable theoretical model for analogous coordination compounds. The observed emission dissymmetries were compared with TDDFT predicted values. The results confirmed viability of the model for other coordination compounds, providing realistic emission dissymmetry values [34(b)]. Helicenes have been reported as systems with a particularly large CPL response [35], similarly as for ECD. Recently, platinahelicenes with a large spin–orbit coupling constant present in non-stereogenic platinum atom exhibited a circularly polarized phosphorescence of a very high-*g* value, 10^{-2} [36].

Kaizaki and Muller reported an extraordinary large CPL intensity for a tetrakis((+)-3-heptafluorobutylyrylcamphorato)Eu(III) complex with an encapsulated Cs^+ ion, comprising $Cs^{I}\cdots FC$ (fluorocarbon) interactions [37]. The absolute maximum value of the luminescence dissymmetry factor *g* was 2, higher than in previously reported CPL of lanthanide complexes in solution. They extended ECD and CPL studies to a series of analogous lanthanide complexes with encapsulated alkali metal ion [38]. The large CPL signal of the 4f–4f transitions carried rich information about stereospecific formation of chiral Ln(III) complexes. The ECD spectra reflected a helical arrangement of chelated ligands. The 4f–4f ECD–CPL spectra in the hypersensitive transitions revealed an empirical spectra/structure correlation for the optical activity of lanthanide complexes.

2.3. Vibrational circular dichroism (VCD)

Compared with ECD, the vibrational techniques provide more local structural information, seeing interactions through covalent bounds or short-range electromagnetic interactions. The application of VCD to determination of the absolute configurations in organic chemistry has been promoted by the development of the quantum-mechanical theory of VCD intensities, and its implementation using ab initio density functional theory [39]. VCD was applied to correct the X-ray absolute configuration assignments of conformationally flexible molecules [40].

Early VCD investigations of metal complexes revealed the chelate ring conformation of transition metal complexes [41]. In 2001, Nafie et al. reported the first ab initio VCD calculation for a coordination compound, closed-shell Zn(II) complex of 6*R*, 7*S*, 9*S*, 11*S*-(−)-sparteine. The simulated and experimental IR and VCD were quite close [42]. For open-shell Co(II) and Ni(II) complexes (Fig. 11), VCD intensities are enhanced if compared with the Zn(II) species. These studies confirmed that VCD can be applied to coordination compounds as a probe of absolute configuration, optical purity, and solution conformation at the same extent as for the organic compounds.

There is a general belief that VCD is less predictable for open-shell systems [43]. But recent results suggest that the VCD simulations can be also applied to open-shell metal complexes, although potential convergence problems are expected to be more frequent than for the closed shell systems. For example, Sato et al. discussed the impact of the d electrons of metal ions in tris(β-diketonato) metal complexes on VCD shapes (Fig. 12) [44]. Distinctive effect of the central metal ion was observed on VCD peaks of the C—O stretches (1500–1300 cm^{-1}). The DFT

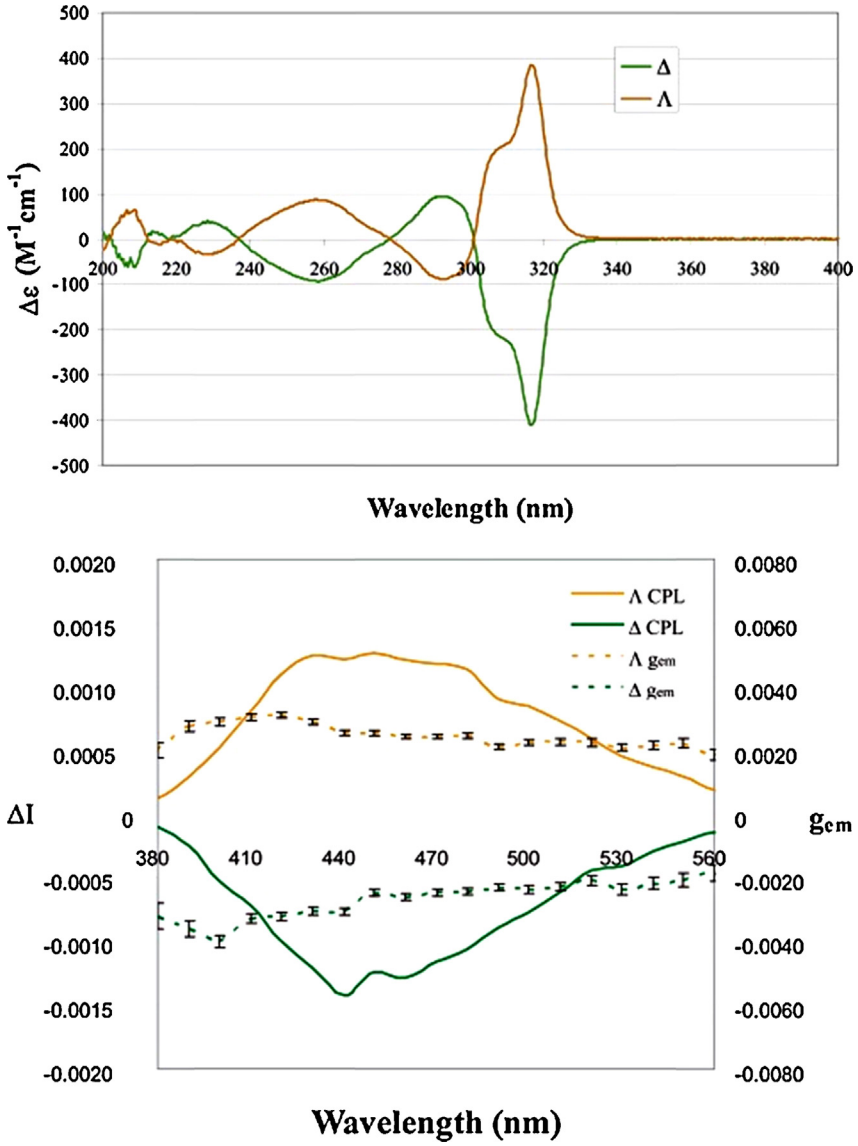

Fig. 9. The experimental ECD (up); and CPL spectra with the emission dissymmetry values (bottom) of Zn(II) hemicage complexes (Δ-configuration, green; and Λ-configuration, orange). Reproduced with permission from Ref. [33]. Copyright 2007 American Chemical Society.

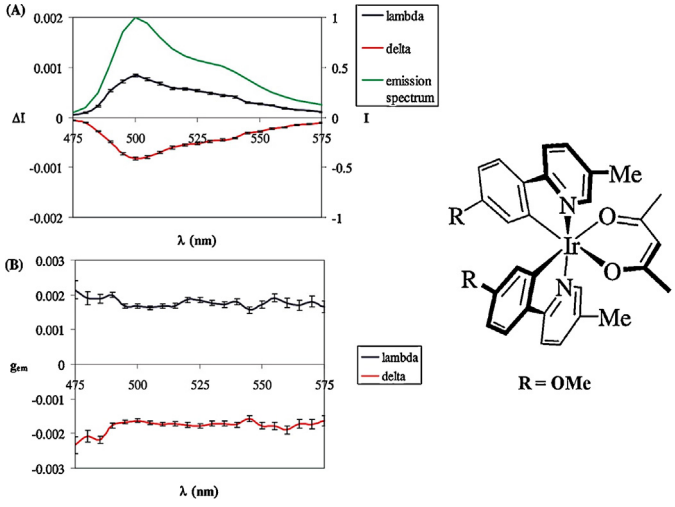

Fig. 10. The emission and CPL spectra (A), and emission dissymmetry (g_{em}) as a function of wavelength (B), for chiral heteroleptic Ir(III) complexes. Reproduced with permission from Ref. [34(b)]. Copyright 2008 American Chemical Society.

calculation approximately reproduced VCD of Co(III), Rh(III), and Ir(III) complexes, but failed in predicting spectra of Ru(III) and Cr(III) complexes. This discrepancy was attributed to the open-shell properties of these metals, and open-shell TDDFT calculations with all-electron scalar relativistic treatment were performed, to analyze VCD spectra of [M(III)(acac)$_3$] (M = Cr, Co, Ru, and Rh) [45]. The authors verified that such calculation and the harmonic approximation approximately fitted the experimental result for complexes of Co(III), Rh(III), and Ru(III). For the Cr(III) complex, anharmonic effects should be considered for predicting the accurate vibrational frequencies of close modes.

For open-shell metal complexes, an enhancement of VCD signals may occur due to the existence of a low-lying electronic state. Nafie investigated such VCD enhancement mechanism, and analyzed the role of low-lying excited electronic states in the VCD signal of coordination compounds with d–d transitions [46]. The enhanced VCD signals are quite helpful for the stereo-chemical analysis. For example, Thulstrup reported VCD study of a spin-triplet bis-(biuretato) Co(III) coordination compound [47]. Several strong VCD transitions were observed in both the liquid and solid phases, attributed to the coupling of vibrational and electronic transitions. Cobalt

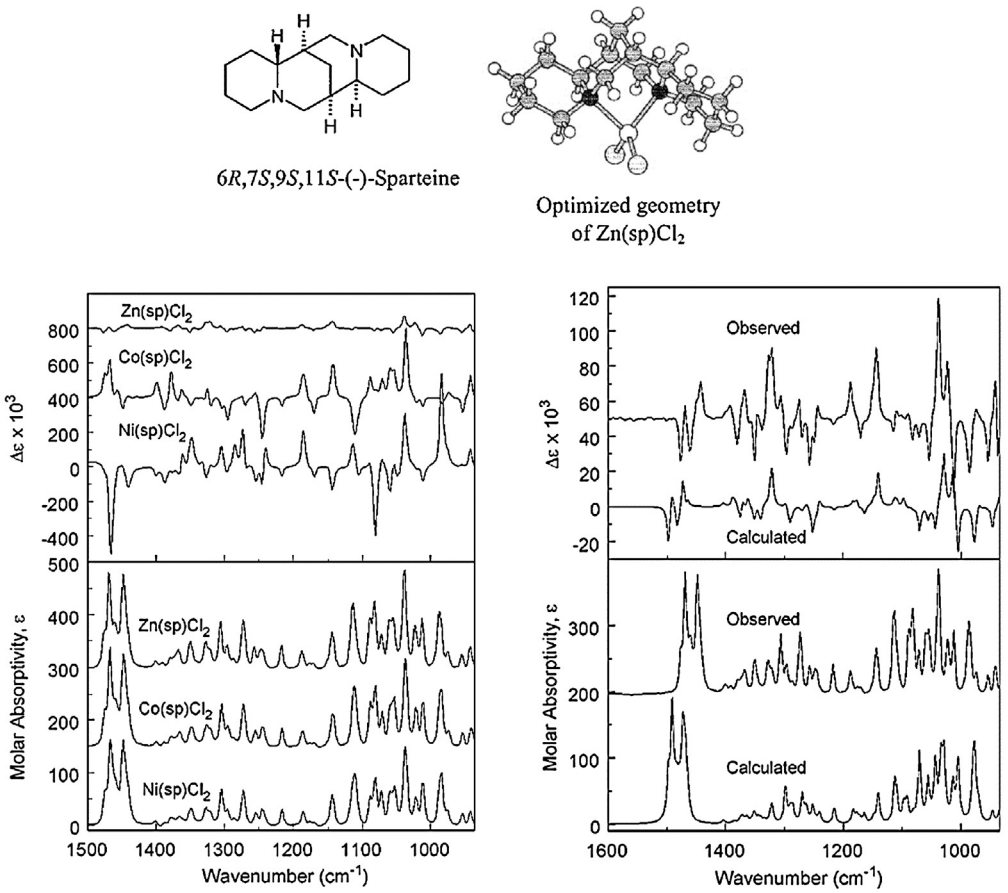

Fig. 11. Experimental VCD spectra of $Zn(sp)Cl_2$, $Co(sp)Cl_2$, and $Ni(sp)Cl_2$ (left) and simulated VCD spectra of $Zn(sp)Cl_2$ (right). Reproduced with permission from Ref. [42]. Copyright 2001 American Chemical Society.

coordination compounds could be used as marker models for active sites. Recently, VCD spectroscopic intensities of amino acids and oligopeptides were enhanced upon coordination with the Co^{2+} ion, which originated in the vibronic coupling and a participation of low-lying electronic states [48].

Nafie et al. also performed a series of experimental and theoretical studies on VCD spectra of coordination compound $[Co(en)_3]^{3+}$ [41(c),49]. The recorded VCD signals both in the hydrogen stretching and mid-infrared regions were sensitive to the nature and concentration of the halide counterion. TDDFT calculations confirmed the absolute configuration assignment [49]. Major ring conformation in solution was derived from VCD features, characteristic of an en-ring conformation, and a mode associated with the chloride ion.

Nicu et al. revealed that the donor–acceptor interactions between the Cl^- base and the N—H σ^* acceptor orbitals encountered in the complexation of Cl^- counterions to the $[Co(en)_3]^{3+}$, led to a large enhancement (between 1 and 2 orders of magnitude) of

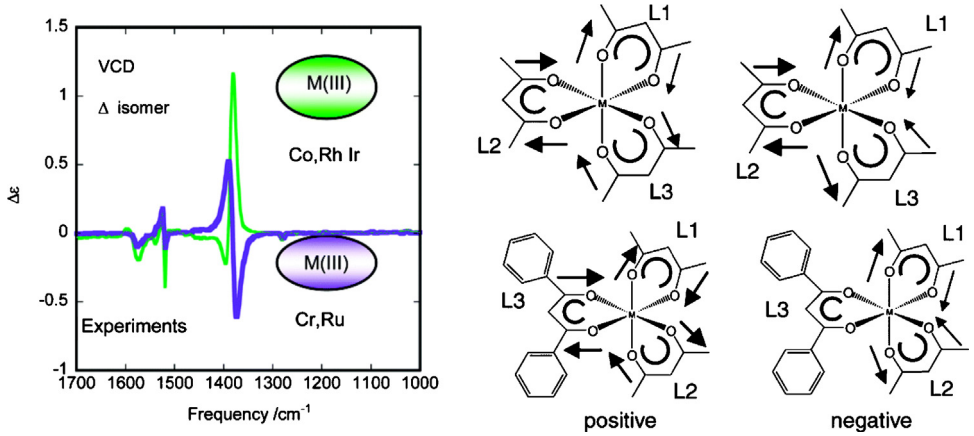

Fig. 12. Study documenting and analyzing the impact of d electrons of metal ions in tris(β-diketonato) complexes on VCD shapes. Reproduced with permission from Ref. [44(b)]. Copyright 2007 American Chemical Society.

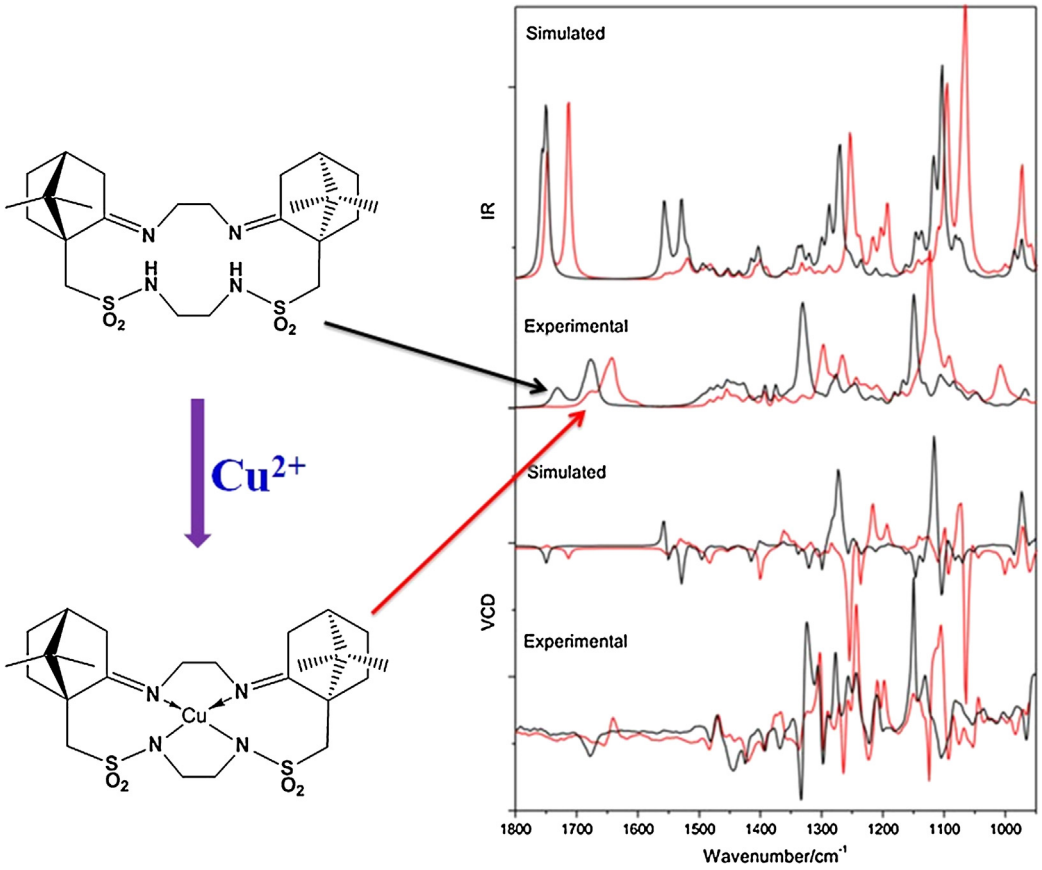

Fig. 13. Copper(II) coordination with a chiral ligand monitored by VCD [21(d)].

the VCD intensities of N—H stretching modes [50]. They attributed this enhancement to the charge transfer from the chloride ions to the N—H bond.

Di Bari et al. proposed that lanthanide ions could cause a shape-conserving enhancement of VCD spectra, i.e. the positions and relative amplitudes of the bands are conserved, which they termed as a lanthanide induced VCD enhancement (LIVE) [51]. Unlike VCD enhancement caused by the charge transfer, LIVE was influenced by the nature of Ln^{3+} only, and not by the coordinating ligated anion. Such enhancement is helpful for understanding of the chirality features of lanthanide complexes in solution, for design of NMR shift reagents, etc.

Chiral oxorhenium(V) complex has a relatively simple chemical structure, which plays a key role in fundamental physics as a potential probe for molecular parity-violation (PV) [52]. Crassous et al. scanned the VCD spectra of several enantiopure chiral oxorhenium(V) complexes [53]. Despite the fact that the rhenium atom did not act as a stereogenic centre, the surrounding chiral environment was responsible for the VCD signal. With the support of quantum chemical calculations, they concluded that VCD spectroscopy is an excellent technique for (potential) monitoring PV effects.

Dinuclear rhodium(II) complexes are important because they exhibit catalytic activity at asymmetric catalysis, and were proposed as anticancer agents. Szilvágyi et al. employed VCD spectroscopy for conformational studies of chiral amino acids derived dinuclear rhodium(II) complexes [54]. The calculated VCD spectra of the conformers were in a good agreement with the experimental results. The exciton coupling effect of the C=O groups [55] was important for the determination of absolute configuration [56].

Janiak et al. investigated diastereoselections of pseudotetrahedral zinc-Schiff base complexes in $CDCl_3$ solution [57]. Not only the absolute configuration could be assigned based on the comparison between experimental and calculated VCD spectra, but the sensitivity of VCD signal to the metal-centered Δ/Λ-chirality was reflected by a feature band characterizing coupled vibrations of the two ligand's C=N stretch modes. Xu et al. reported that VCD spectra were able to reflect the influence of the electron configuration and coordination number of coordination compounds based on *trans*-1,2-diaminocyclohexane (chxn) [58]. They also examined associated VCD spectra of homo- and heteroleptic geometries when one chxn in $[Cu(chxn)_3](ClO_4)_2$ was replaced with another ligand [59]. Comparison with the calculated spectra revealed that the spectroscopic differences are associated with the relative abundances of the Δ- and Λ-configurations. VCD signals of the NH_2-bending modes were independent on the coordination number and the configuration of the metal centre. Lately the same authors investigated solvent impact on the equilibrium between Δ and Λ stereoisomers of a tris(diamine)nickel(II) complex [60]. Significant shift of the equilibrium towards the Λ diastereomer was observed for the complex in dimethyl sulfoxide. In a VCD characterization of optically active tripodal dendritic polyoxometalates (POM) [61], predicted intensities of P—O and W=O stretching vibrations reflected the chirality transfer from the ligand to the POM cluster.

Chiral metal complexes with π-bonded ligands (such as chiral metallocene etc.) are an important group of asymmetric catalysts. Unlike most δ-bonded metal complexes where the metal ions function as the stereogenic centres, most π-bonded metal complexes are planar. Stephen et al. reported the experimental and theoretical VCD studies of a chiral tricarbonyl-η^6-arene-chromium(0) complex [62]. Merten et al. examined the influence of different central ion and counterion on VCD spectra of a Ziegler–Natta-catalyst, dichloro[(*S*,*S*)-ethylenebis(4,5,6,7-tetrahydro-1-indenyl)] zirconium(IV) [63]. These results show that VCD spectroscopy is

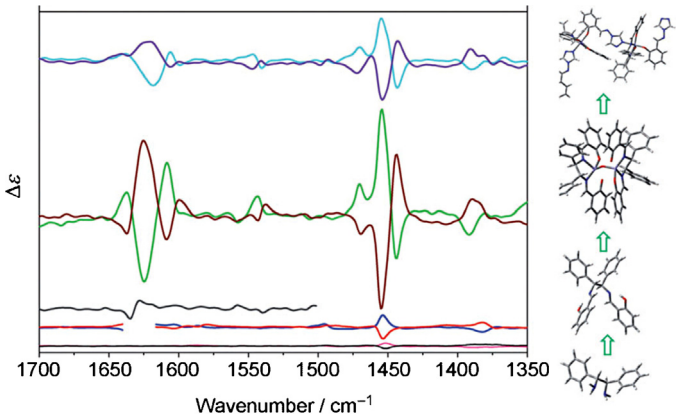

Fig. 14. VCD spectra monitoring the polymerization process, from bottom to top: chirality-pool diamine, Schiff base ligand, dinuclear iron(III) complex, and 1D iron(III) coordination polymer [69].

valuable for the design and structural analysis of asymmetric catalysts based on metal complexes.

Kaizaki et al. examined the comparable VCD spectra for a series of eight coordinated tetrakis((+)-3-heptafluorobutylyryl-camphorato)Ln(III) complexes with an encapsulated alkali metal ion. In comparison with the DFT calculations and previous ECD and/or CPL studies, the most intense VCD shapes near 1550 cm^{-1} changed under alteration of the central lanthanide(III) ion [64]. The VCD signal intensified as the ionic radius of alkali metal ion increased, from K^+ to Cs^+. VCD spectra were almost unchanged with different lanthanide ions, which were in consistent with ECD observation. No influence of low-lying electronic states observed in these Eu(III) species. For a series of Cs+ ion related lanthanide(III) complexes VCD intensities were strongly linked with the parity of the total orbital angular momentum *L* in the ground state terms of Ln(III) ions [65]. VCD spectra were not capable, however, of distinguishing between the ground state electron configurations and spin multiplicities.

Recently Sato et al. extended VCD spectroscopic explorations to the oligomers of β-diketonato complex frameworks [66]. By comparing the VCD spectra of eight diastereomeric enantiomers of these star-burst type tetranuclear Ru(III) complexes, the homo- or hetero-chiral character of the bridging part linking the central core and the peripheral skeleton could be discriminated. VCD spectroscopy could manifest the static and dynamic properties of mononuclear and multinuclear optically active metal complexes, not approachable by other spectroscopies [67].

Lately, we obtained two novel species of enantiomeric transition metal coordination compounds with predetermined configuration via macrocyclic ligands derived from camphor [21(d),68] (see also Fig. 1). Similarly as for ECD, VCD could serve as an excellent technique to monitor the coordination process in copper(II) complexes [21(d)] (Fig. 13). Analogously, a chirality transfer in a magnetic coordination polymer was accompanied by the VCD exciton coupling phenomena [55] of the ligands in the iron(III) complex or polymer (Fig. 14) [69]. VCD was capable of detecting subtle variances of chirality in small biologically active systems containing metal, useful for probing chiral recognition in coordination compounds [70]. Through the stereo-chemical analysis of the racemization of a chiral bipyridine coordinating with metal ion VCD detected the enantiomeric excess during the coordinating process [71].

Poly(pyridylamide) ligands are generally used for building molecular wires. But these extended metal atom chains are normally isolated as racemic crystals. Cotton et al. established an approach for exploring the chirality of such-type molecular wires

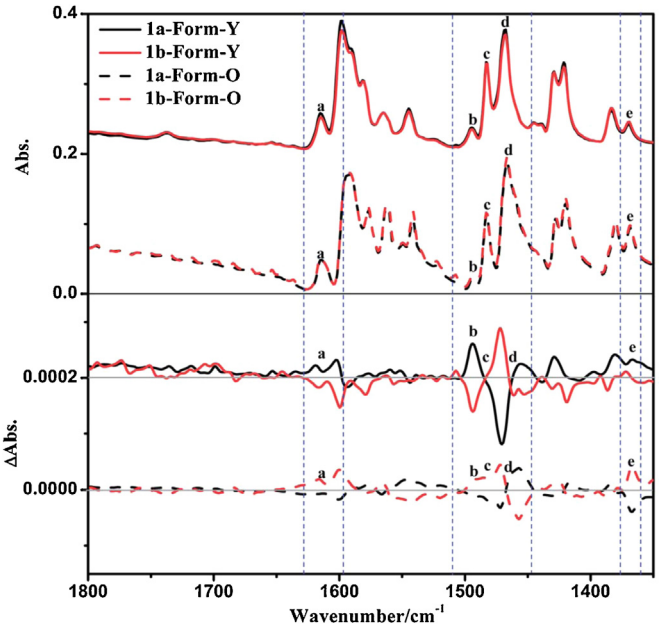

Fig. 15. Solid state IR (up) and VCD spectra (bottom) (fluorolube mull) of two polymorphs (Form-Y and Form-O) of crystalline cyclometalated platinum(II) complexes [75(b)].

by VCD, ECD and ORD methods with the aid of DFT calculations [72]. Despite a few bands influenced by the strong absorption of solvent, VCD provided more information on the helical structure when compared with ECD and ORD. The discrepancies of wavelength shifts for electronic transitions between experimental and calculated spectra of ECD and ORD, however, could not be reconciled by current DFT methods.

CD spectroscopy is usually applied for solutions. Solid state species may cause sample anisotropy. Additionally, solid state UV–vis measurement is more difficult than IR measurement. Artefacts may destroy recorded spectra, depending on the sample [73]. VCD for solid-phase samples is available in KBr pellets or as a suspension of a powder in fluorolube/mineral oil. In spite of the artefacts due to the inhomogeneous/non-isotropic sample, solid state VCD [47,68,74] was valuable for the stereo-chemical analysis of coordination compounds (particularly for coordination polymers). Many crystalline samples are not stable in solution or accessible by other spectroscopic methods. For example, crystals of cyclometalated platinum(II) complexes exist in many polymorphic forms.

We designed and synthesized several groups of enantiopure cyclometalated platinum(II) complexes [75]. A series of samples were prepared and measured under the same conditions to avoid artefacts. Then the crystalline-to-amorphous transformation upon mechanical grinding [75(a)] and single-crystal-to-single-crystal transformation upon vapour exposure [75(b)] could both be monitored by solid state VCD (Fig. 15). The results were consistent with solid state ECD measurements. The single-crystal-to-single-crystal transformation was further confirmed by single crystal X-ray diffraction [75(b)].

2.4. Vibrational Raman optical activity (ROA)

Compared with VCD, vibrational ROA spectroscopy is less common. ROA is less sensitive than VCD and requires larger sample amounts, but it comprises larger spectroscopic region. Unfortunately, water as the most convenient solvent for a ROA is not suitable for most coordination compounds. Additionally, many samples exhibit fluorescence during the measurement with the

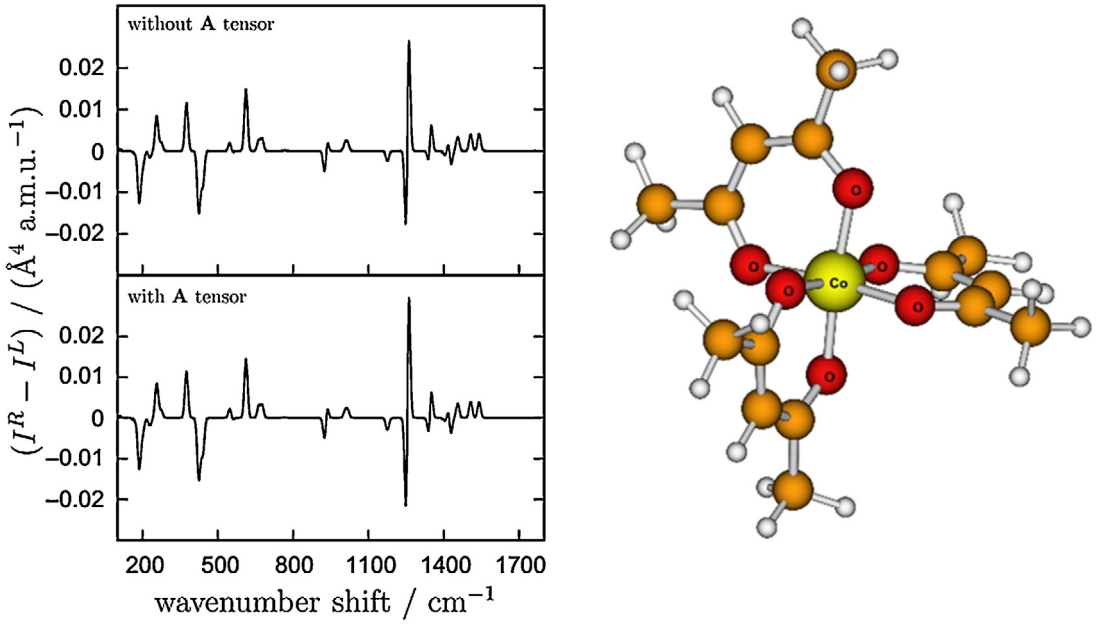

Fig. 16. Calculated backscattering ROA spectrum (BP86/RI/TZVPP) of Λ-tris(acetylacetonato)cobalt(III): upper, without the **A** tensor contribution; lower, full reference spectrum [76]. Reproduced with a permission of Elsevier.

green 514 or 532 nm lasers. Reiher et al. reported the first theoretical analysis of ROA spectra of chiral metal complexes (Fig. 16). Their calculations suggested that in spite of the practical problems ROA is a very sensitive tool discriminating between metal complexes differing in the central metal ion [76], and between the Δ and Λ configurations, in addition to the chirality of the ligand(s) [77].

The first ROA measurement of a coordination compound was reported by Merten et al. with a lanthanide complex (+)-tris[3-trifluoroacetyl-D-camphorato]europium(III) [78]. Electronic resonance appears between the laser light (532 nm) and the $^7F_1 \rightarrow {}^5D_1$ transition of the Eu^{3+} metal centre. Natural non-resonant ROA spectra of coordination compound were observed later by a chiral zirconium(IV) complex, and reproduced by theoretical calculations [79].

The circular intensity difference (ratio of the ROA and Raman intensities) is expected to be enhanced in the induced resonance ROA of in Eu(III) complex. Recently, Yamamoto and Bouř employed this strategy for sensitive chirality detection of optically active alcohols and ketones by chelating them with an achiral europium complex (Fig. 17) [80]. These experiments combine ROA with circularly polarized luminescence.

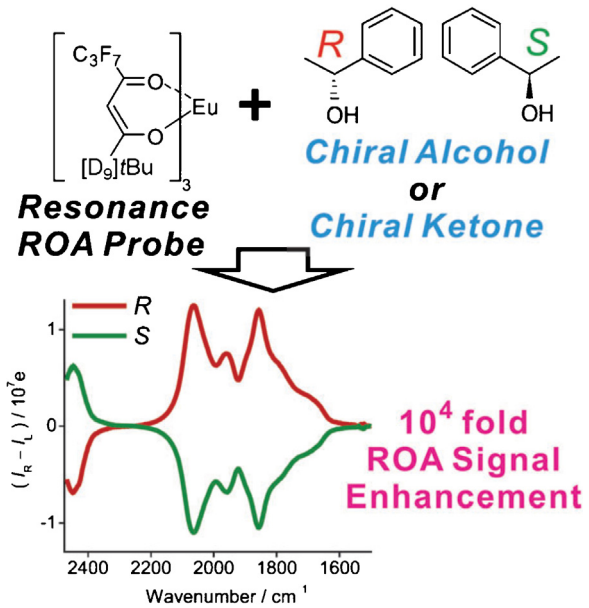

Fig. 17. Induced resonance Raman optical activity (IRROA) in the presence of a europium complex enabled the detection of molecular chirality with a 10^4-fold increase in sensitivity relative to that observed with conventional nonresonant vibrational ROA [80].

3. Applications of chiral coordination compounds

3.1. Second-order nonlinear optic (NLO) materials

Second-harmonic generation (SHG), one of the most popular NLO characteristics, is broadly applied in optical devices and information technologies (Fig. 18). Coordination compounds appeared as a new family of NLO materials due to their specific features such redox and magnetic properties, and variable geometries [81]. The absence of the centre of symmetry is sufficient for SHG-active material. Noncentrosymmetric metal-organic frameworks (MOFs) are ideal platforms for design and preparation of SHG materials, because of the metal centres, tailored geometry, and privileged metal-ligand coordination interactions [9(a)]. In particular, noncentrosymmetric MOFs sharing a diamond structure appear as very handy topological blocks.

In principle, all chiral crystals should be SHG active. Since chiral molecules crystallize in chiral space groups, assembling coordination compounds with enantiopure ligands seems to be a straightforward approach to construction of an SHG-active material (Table 2). However, SHG activities in individual compounds vary strongly. Note that the process of SHG material design can be enhanced by theoretical predictions, similarly as the (V)CD/CPL/ROA spectroscopic analyses.

Lately, pinene-derived enantiopure bipyridines [82,84] and tripyridines [83] were employed to assemble zero-dimension (0-D) coordination compounds with lanthanide ions, displaying a stronger SHG activity. A strong enhancement of the SHG response

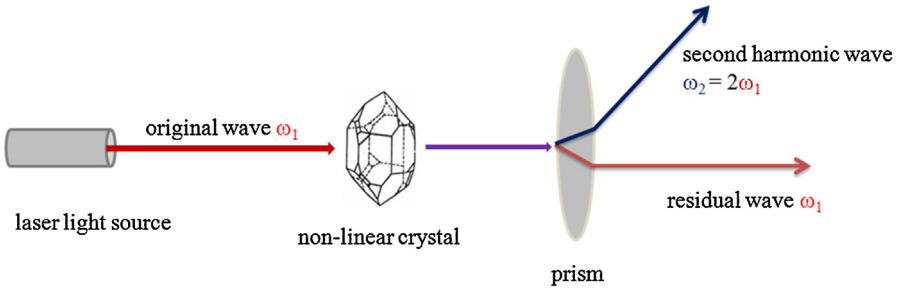

Fig. 18. The second-harmonic generation process.

Table 2
Selected SHG-active chiral coordination compounds.

Compound	Chemical formula	Dimension	Space group	SHG ($I^{2\omega}$)	Refs.
1	$[Eu(tta)_3pbpy]$	0-D	$P2_1$	5 × Urea	[82]
2	$[Eu(tta)_3(dptp)](C_3H_6O)\cdot 0.5\,H_2O$	0-D	$P2_1$	0.9 × Urea	[83]
3	$[Eu(bta)_3(dptp)](C_3H_6O)$	0-D	$P2_12_12_1$	0.1 × Urea	[83]
4	$[Dy(L_1)_2(acac)_2]NO_3\cdot CH_3OH\cdot H_2O$	0-D	$P2_1$	6 × KDP	[84]
5	$\{[Dy(L_1)_2(acac)_2]NO_3\}_2\cdot 0.5\,H_2O$	0-D	$C222_1$	1 × KDP	[84]
6	$[(NiL^1)_2\text{-}Na]^+NCS^-\cdot MeOH\cdot Et_2O$	0-D	$P2_1$	0.8 × Urea	[85]
7	$[Zn(bddp)\cdot(H_2O)_4]_2\cdot H_2O$	1-D	$P2_1$	0.6 × Urea	[86]
8	$[Cd(L\text{–}N_3)_2(H_2O)_2]_n$	1-D	*Aba*2	80 × Urea	[87]
9	$Cd(D\text{-}ca)(bte)\cdot H_2O$	2-D	*Aba*2	0.3 × Urea	[88]
10	$Cd_4(D\text{-}ca)_4(btp)_2(H_2O)_4$	3-D	$P2_1$	0.8 × Urea	[88]
11	$Cd(D\text{-}Hca)_2(bth)(H_2O)\cdot H_2O$	3-D	*P*1	0.4 × Urea	[88]
12	$Zn_2(etza)_4$	3-D	$P2_1$	0.6 × Urea	[89]

was found in a 1-D polymer with Cd^{2+} ion coordinated with a ligand containing multi-chiral centres [87]. The SHG signal was more than 80 times higher when compared with urea.

For the 0-D coordination compounds listed in Table 2 [82–85] the chirality was explored by ECD spectra. The coordination polymers [88,89] provided solid state VCD spectra. For coordination polymer **12** [89] constructed from achiral building blocks, solid state VCD provided confirmation on the enantiomeric excess.

3.2. Ferroelectric materials

Ferroelectric materials are a class of dielectrics and a sub-unit of pyroelectrics and piezoelectrics manifesting spontaneous electric polarization. Its direction can be reversed by external electric field. Chiral ferroelectrics simultaneously share pyroelectricity and piezoelectricity, as well as SHG properties, which enables many applications in molecular electronics. Ferroelectric materials crystallize in 10 polar point groups, C_1, C_s, C_2, C_{2v}, C_3, C_{3v}, C_4, C_{4v}, C_6, and C_{6v} [90,91]. So far more than 300 ferroelectric compounds have been investigated [9(b)].

Lanthanide cations are generally employed to tune properties of ferroelectrics, such as the lead zirconium titanate (PZT) for obtaining high remnant polarization (P_r) values, square hysteresis loops, and enhanced fatigue resistance [92]. In addition, a square-antiprism geometry distortion can bring intensive charge separation to induce ferroelectric effect, similar to non-H-bonded ferroelectrics $TiBaO_3$ [93]. Enantiopure europium complex **1**, $[Eu(tta)_3pbpy]$ (tta = 2-thenoyltrifluoroacetonate); pbpy = (−)-4,5-pinene bipyridine, or (+)-4,5-pinene bipyridine) crystallized in chiral space group $P2_1$ belonging to C_2 polar point group was obtained by employing chiral 2, 2′-bipyridine as the asymmetric factor [82]. The ferroelectric value measured on thin film ($Pr \approx 0.022\ \mu C\,cm^{-2}$) (Fig. 19) is significantly improved compared with the pellet sample ($Pr \approx 0.006\ \mu C\,cm^{-2}$).

Ionic coordination compounds are more effective in polarity and ferroelectricity than neutral molecules. An enantiomeric pair of ionic trinuclear alkali-metal complexes belonging to C_2 polar point group (space group, $P2_1$) was collected by using optically active Schiff base ligands [85]. The value of *Pr* is ca. 4.18-5.33 $\mu C\,cm^{-2}$ and saturation spontaneous polarization is ca. 6.15-9.41 $\mu C\,cm^{-2}$ larger than for a typical inorganic ferroelectric KH_2PO_4.

For chiral coordination compounds it is more difficult to explain the ferroelectric origins than for traditional materials, due to their complicated structure [90,93]. Possible mechanisms may incorporate geometrical distortion near the metal centre and motion or distortion of the counterions. The chirality of the ferroelectric coordination compounds can be monitored by ECD and VCD in the same way as for SHG materials.

3.3. Chiral molecular conductors

A combination of chirality and conductivity in many materials lead to electrical magneto-chiral anisotropy. The external magnetic field is parallel to the direction of the current. The anisotropy was predicted and observed also in chiral nanotubes by Rikken and co-workers [94].

The chiral Hall effect is another interesting phenomenon, when the external magnetic field is perpendicular to the current [95]. Most molecular conductors are prepared on the basis of tetrathiafulvalene (TTF) derivatives [96]. In TTF-based metal complexes, there might be a strong coupling between the localised d electrons (coming from the metal centre) and the mobile π electrons (coming from the TTF), which provides a significant way to prepare multi-properties materials [96(b)].

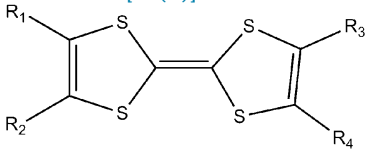

tetrathiafulvalene (TTF)

An enantiopure semiconductor employing $Sb_2((2R, 3R)\text{-}(+)\text{-tartrate})_2$ as the optically active inductor anion through electrocrystallization was made by Coronado and co-workers [97] (Fig. 20).

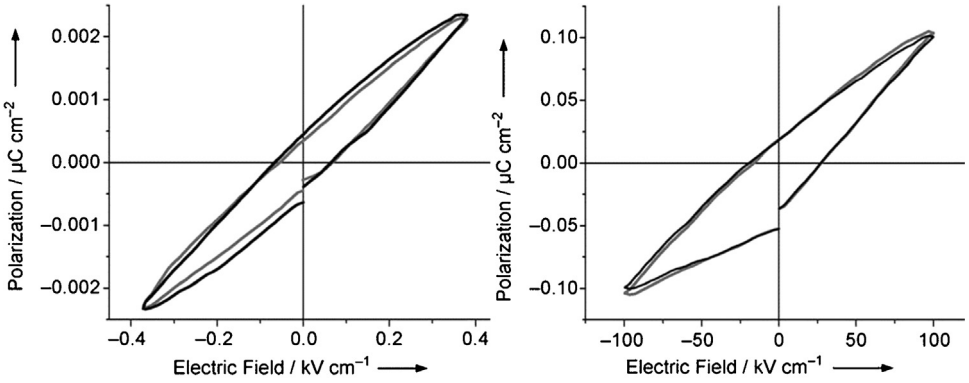

Fig. 19. Polarization hysteresis loops of europium complex **1** on powdered samples (left) and on thin films (right) [82].

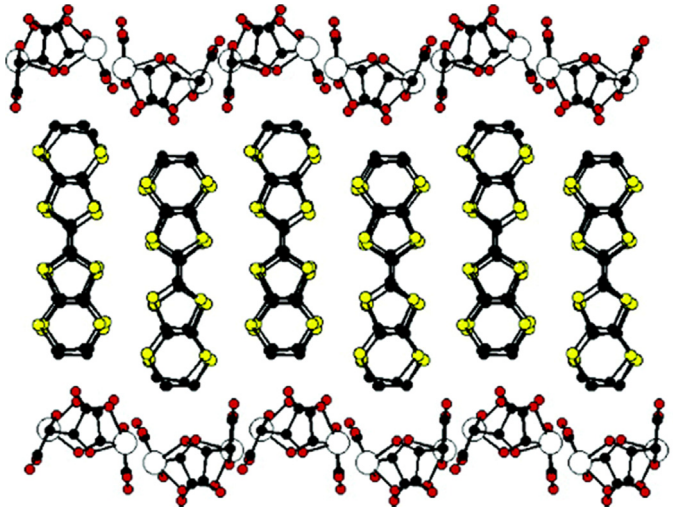

Fig. 20. Alternating layers in the $[ET]_3[Sb_2(L\text{-tart})_2]\bullet CH_3CN$ salt (ET = bis(ethylendithio)tetrathiafulvalene; L-tart = (2*R*, 3*R*)-(+)-Tartrate). Reproduced with permission from Ref. [97]. Copyright 2004 American Chemical Society.

It crystallizes in the $P2_12_12_1$ space group, and is composed of one anionic and one cationic network in alternate layers. In the solid state ECD spectrum, a signal below 240 nm was attributed to the organic part related to the conducting lattice. The spectrum of the semiconductor salt confirmed that the overall chirality of the crystal influences the organic radicals, despite the symmetry of individual molecules.

Several reports revealed that the conductivity of molecular conductors based on coordination compounds in the enantiopure state could be strengthened if compared with the racemate [98–100]. For chiral TTF-derivatives, chiroptical spectra revealed valuable conformation in solution [101].

3.4. Chiral molecule-based magnets

Coordination chemistry also contributed to the development of molecule-based magnets [102]. Molecular magnetism can coexist or interact with other physico-chemical properties [103], which is helpful for manufacturing of multi-functional materials. Distinct physical properties are also obtained by integration of the chirality and magnetism [10,104]. Enantiomeric chiral magnets (ECM) has drawn the interest of both chemists and physicists because of the forecast [105] and detection of a cross-effect in paramagnetic [106] and diamagnetic [107] enantiopure systems.

The combination of Faraday effects and circular dichroism is referred to as the magneto-chiral (MCh) effect. It is proportional to the magnetization, and its intensity was predicted to be profoundly promoted in ECM. The light source used for measuring magneto-chiral dichroism (MChD) emits unpolarized light, as opposite to the circularly polarized light in CD (Fig. 21).

In molecular magnetism, a long term goal is to store and read information stored on a single unit like single-molecule magnet (SMM) [108] or single-chain magnets (SCM) [109]. MChD might be applied to detect for systems incorporating enantiopure SMM [110] and SCM [111].

Train et al. synthesized a 2D bimetallic oxalate bridged framework in two enantiomeric forms, by employing a tetraalkylammonium countercation with a chiral carbon on one alkyl chain as a template (Fig. 22) [104]. This material manifested fascinating magnetic properties, including an abrupt paramagnetic-to-ferromagnetic phase transition at 7 K. A strong MCh effect was detected for the first time on this ferromagnet. The MCh values in the ferromagnetic phase were 17 times larger than that in the paramagnetic case. This work thus perhaps opens the magneto-chirality phenomena to data storage applications.

Lanthanides have a special position in magnetism because of their large magnetic moments and generally distinct magnetic anisotropy [112]. The magnetic anisotropy facilitates construction of SMM [113]. It is expected that adding the chirality to lanthanide-based SMM would transfer the asymmetry to the ligand field, which is crucial for dynamic magnetism. A C_3-symmetric, square-antiprismatic β-diketonate complex [Dy-$(FTA)_3$(BBO)] (FTA = 2-furyltrifluoro-acetonate, BBO = (*S*,*S*)-2,2′-bis(4-benzyl-2-oxazoline)) (**14**) was synthesized by introducing chiral oxazoline as a co-ligand [114]. The chirality was indicated by the ECD spectra. It exhibited slow magnetic relaxation and SMM behaviour.

4d and 5d orbitals are more diffuse than 3d orbital, which enables a stronger magnetic exchange coupling to surrounding ions. Recently Zuo et al. reported chiral SCM of cyano-bridged Ru^{III}–Mn^{III} heterobimetallic chains assembled by versatile chiral cyanometallic units ((*R*,*R*) or (*S*,*S*))-$[Bu_4N][Ru(5\text{-Cl-Salcy})(CN)_2]$ [115]. Strong antiferromagnetic coupling between Ru^{III} and Mn^{III} centres linked by cyanide was observed. Both enantiomers behaved like single-chain magnets. Solid state VCD was applied to confirm the enantiomeric properties of crystalline coordination polymers (Fig. 23).

3.5. Multi-functional materials

Because of the cross-effects like MChD, enantiopure chiral magnets can be viewed as splendid examples of multi-functional molecule-based materials. Combination of two properties gives birth to the third one. The absence of centrosymmetry necessary

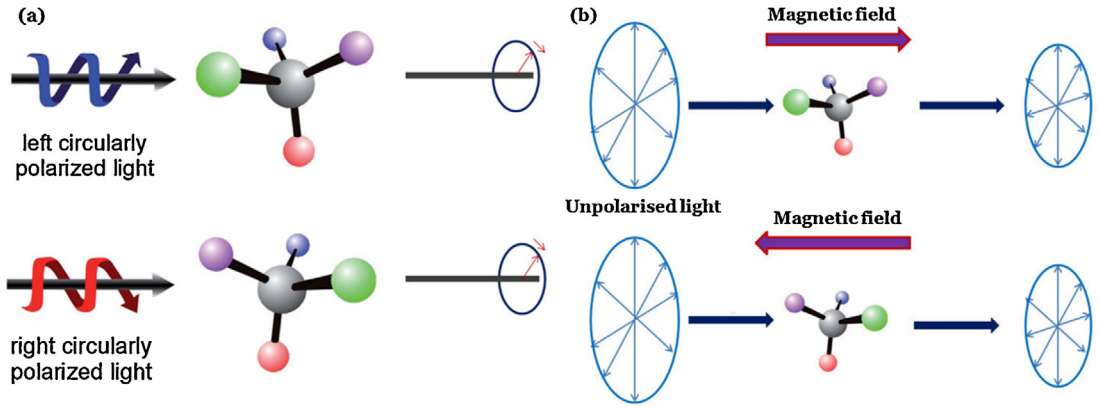

Fig. 21. A comparison between CD (a) and MChD (b).

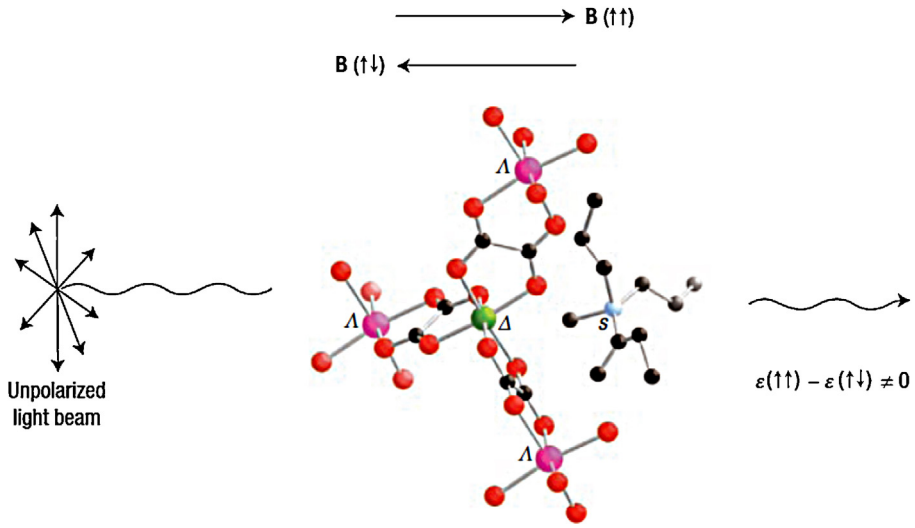

Fig. 22. MChD in a chiral ferromagnet [N(*S*)-(CH_3)(*n*-C_3H_7)$_2$(*s*-C_4H_9)]$^+$[(Λ)-Mn^{II} (Δ)-Cr^{III} (ox)$_3$] **13**. (Mn(II) ion in pink and Cr(III) ion in green). Reproduced with permission from Ref. [104(a)]. Copyright 2008 Nature Publishing Group.

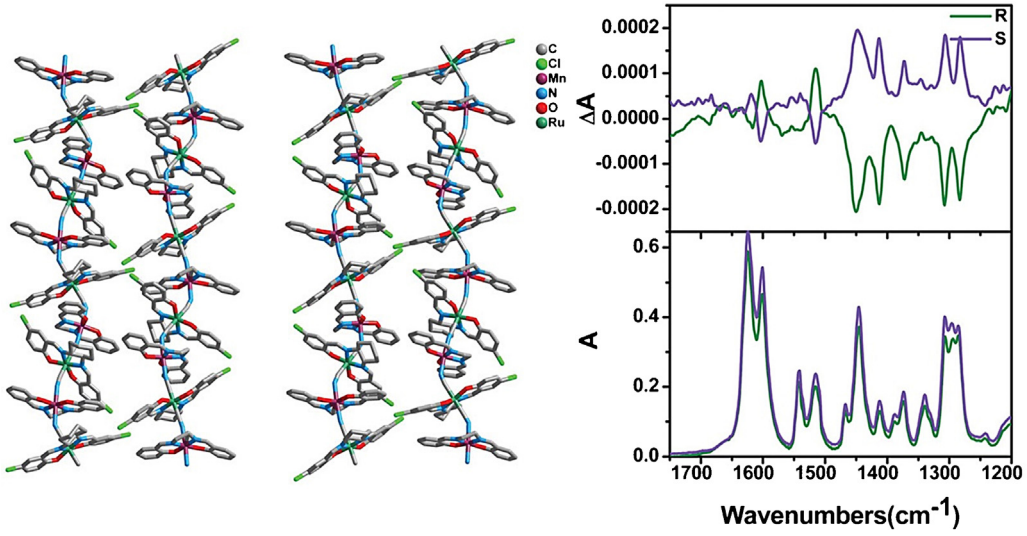

Fig. 23. Structures of 1-D zigzag Ru^{III}–Mn^{III} heterobimetallic chains derived from ((*R*,*R*) (left) and (*S*,*S*))-[Bu_4N][Ru(5-Cl-Salcy)$(CN)_2$] (right), and their measured solid state VCD and IR spectra in KBr pellets [115].

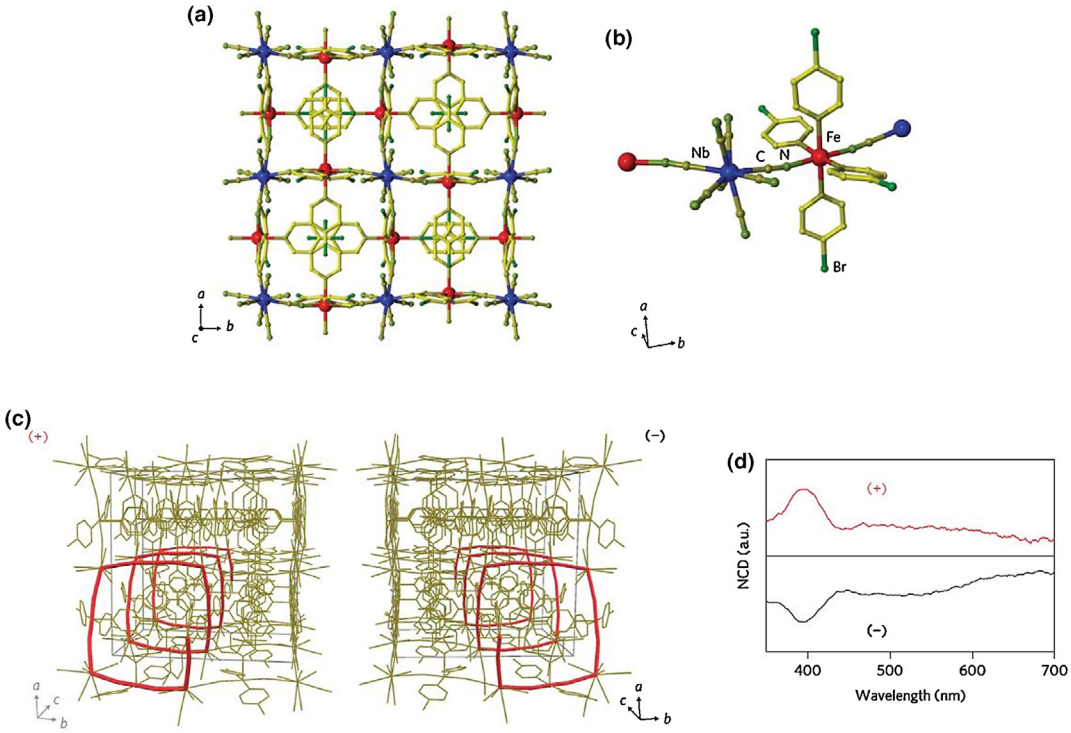

Fig. 24. Crystal structure of magnet coordination compound (+)-$Fe_2[Nb(CN)_8](4\text{-bromopyridine})_8.2\,H_2O$ (**15**). (a) Crystal structure viewed along the *c*-axis; (b) coordination environments around Fe and Nb; (c) the helical spheres along the four-fold screw axis (*c*-axis) of the (+)- and (−)-enantiomers and (d) ECD spectra of the enantiomers. Reproduced with permission from Ref. [120]. Copyright 2014 Nature Publishing Group.

to optical activity is accompanied by unique optical and electric properties [9,10,116].

The SHG signal from a symmetry breaking at an interface can be intensified when the material reaches its ferrimagnetic phase. The changes are associated with the field-cooled magnetization [117,118]. However, the spontaneous change cannot be controlled. Train and Ohkoshi designed a model based on the chiral magnet of compound **13** (space group, $P6_3$), providing both SHG and magnetization-induced SHG (MSHG) in its ferromagnetic state [119]. MSHG extrema enhanced upon a magnetization reversal at 2 K, providing MSHG along with MChD as an efficient approach to detect the magnetization state of enantiopure chiral magnets.

Optical manipulation of physical properties and functionalities of advanced optical materials is yet another great challenge. Recently Ohkoshi et al. reported a magnet coordination compound **15** of chiral iron-octacyanoniobate (Fig. 24), which can switch the polarization plane of light by 90 degrees upon optical stimulation [120]. The magnet manifested three novel characteristics: spin-crossover-induced SHG, light-reversible spin-crossover long-range magnetic ordering, and photoswitching of MSHG. The enantiopure characters of the (+)- and (−)-compounds were verified by ECD spectra.

Multiferroics, which contain two or more ferroic properties (ferroelectricity, ferroelasticity, ferromagnetism) promise applications in data storage and spintronics [121]. It is not easy to predict a rational strategy for design of such materials, because of the cross-effects of ferroelectricity and ferromagnetism. Reported cases are relatively scarce; an effective strategy is an ECM combing with symmetry breaking consideration [9].

Ionic compounds with large net dipole moments when crystallized in polar space groups might possess distinct ferroelectric properties. Enantiopure ionic lanthanide complex **4**, $[Dy(L)_2(acac)_2]NO_3$ [L = (−)-4,5-bis(pinene)-2,2′-bipyridine], combines ferroelectric, SHG, and slow magnetic relaxation behaviour [84]. The enantiopure characters of ionic complex **4** and its enantiomer were confirmed by solid state ECD spectra. This material also shows reversible single-crystal-to-single-crystal transformation associated with the release or absorption of solvent molecules.

A tricyanometalate-based cluster with enantiopure chiral diamine, $\{(MeTp)_2Fe_2(CN)_6Ni[(1R,2R)\text{-chxn}]_2\}$ (**16**) [MeTp = methyltris(pyrazolyl)borate; (1*R*,2*R*)-chxn) = (1*R*,2*R*)-(−)-1,2-diaminocyclohexane] documents the ferroelectricity and intramolecular ferromagnetic interactions [122]. This compound crystallized in a polar point group (C_2), displaying a ferroelectric hysteresis loop with a remnant polarization (*Pr*) of ca. 0.11–0.32 $\mu C\,cm^{-2}$. It exhibited a coercive field (*Ec*) of ca. 8.5–20 $kV\,cm^{-1}$, and the saturation spontaneous polarization (*Ps*) was about 0.85 $\mu C\,cm^{-2}$. The $\chi_M T$ value grew successively from 2.41 $emu\,K\,mol^{-1}$ at 300 K to a maximum of 3.07 $emu\,K\,mol^{-1}$ at 10 K with temperature cooling. The optical activity and enantiomeric nature were confirmed by solid state ECD spectra.

From the examples above, it is evident that ECD spectroscopy is employed more frequently [82–85,97,104(b),114,115,120,122] than VCD [88,89,115]. However, advantages of the latter are evident, e.g. in characterization of crystalline samples [74,75]. Recently, solid state VCD has been used to detect the linkage control between molecular and supramolecular chirality in the construction of chiral hydrogen-bonded twofold helical assemblies with controlled handedness in the crystalline state [123]. Solid state ECD can also be applied to monitor the conglomerate crystals of achiral molecules [124].

Assemblies of advanced molecular materials may provide a helical coordination when enantiopure chiral ligands are employed as building blocks. For achiral or racemic ligands a meso compound, conglomerate of chiral crystals, or spontaneous macroscopic chirality may appear [125]. In such case, solid state CD can also provide a valuable way to test the chirality of the bulk, or individual crystal components. Finally, we should mention the use of chirality in

special cases such as asymmetric catalysis [3(b)], nanoparticles [126] and chiral metal complexes in biochemistry [127].

4. Conclusions and perspectives

Chiroptical spectroscopies are powerful tools for probing the chirality in coordination chemistry. Each technique is sensitive to different structural aspects. All optical spectroscopies are somewhat biased to solution samples, less prone to spectroscopic artefacts, although solid state measurements are also possible.

The electronic circular dichroism spectroscopy is useful in the stereo-chemical analysis of the ground states geometry. When combined with TDDFT calculations, it can be used for the absolute configuration assignment. Circularly polarized luminescence is more suitable as a probe of the excited states, although it has been so far limited to lanthanide complexes.

Applications of vibrational circular dichroism have gradually expanded during the past two decades. VCD usually provides richer structural information than ECD and CPL. ROA explores the same vibrational transitions as VCD, but the technique is more complex. Both methods require a significant instrumental improvement for more routine measurements.

Chiral coordination compounds offer a multitude of electron configurations and geometrical structures. The incorporation of an electron charge transfer or spin order in a chiral material is of interest owing to potential applications in high density magnetic storage, memory, sensors and spintronics. For example, chiral magnets represent a challenge for both chemically and physically oriented scientists. However, much work remains to be done to fully explore the combination of chirality and the magnetic properties.

The preparation of multi-functional materials such as multiferroics is an equally demanding task, in spite of considerable advances in the field. For molecular chemists, the diversity of metal ions and chiral ligands opens up immense opportunities. With the aid of chiroptical techniques, they can construct and control chiral transfer in coordination compounds. Finally, they are likely to facilitate development of rationally designed functional systems applicable in diverse industrial fields.

Acknowledgements

The authors are grateful to National Natural Science Foundation of China (91022031 and 21271099), the National Basic Research Program of China (2011CB808704 and 2013CB922102), Grant Agency (13-03978S and P208/11/0105) and Academy of Sciences (M200550902) of the Czech Republic for financial support.

References

[1] G.P. Moss, Pure Appl. Chem. 68 (1996) 2193–2222.
[2] A. von Zelewsky, Stereochemistry of Coordination Compounds, J. Wiley & Sons, Chichester, 1996.
[3] (a) H. Amouri, M. Gruselle, Chirality in Transition Metal Chemistry: Molecules, Supramolecular Assemblies and Materials, J. Wiley & Sons, Chichester, 2008;
(b) E.B. Bauer, Chem. Soc. Rev. 41 (2012) 3153–3167;
(c) J. Crassous, Chem. Soc. Rev. 38 (2009) 830–845.
[4] (a) E.L. Eliel, S.H. Wilen, L.N. Mander, Stereochemistry of Organic Compounds, John Wiley & Sons, Inc., New York, NY, 1994;
(b) W.J. Lough, I.W. Wainer, Chirality in Natural and Applied Science, Blackwell Science Ltd., Oxford, 2002;
(c) H. Yamamoto, E.M. Carreira (Eds.), Comprehensive Chirality, Elsevier Science, New York, NY, 2012.
[5] R. Baková, M. Chergui, C. Daniel, A. Vlček Jr., S. Záliš, Coord. Chem. Rev. 255 (2011) 975–989.
[6] (a) X.Z. You, Structures and Properties of Coordination Compounds, second ed., Science Press, Beijing, 2012 (in Chinese);
(b) E.C. Constable, Chem. Soc. Rev. 42 (2013) 1637–1651.
[7] U. Knof, A. von Zelewsky, Angew. Chem., Int. Ed. 38 (1999) 302–322.
[8] (a) J. Crassous, Chem. Commun. 48 (2012) 9684–9692;
(b) H. Miyake, H. Tsukube, Chem. Soc. Rev. 41 (2012) 6977–6991;
(c) S.E. Howson, P. Scott, Dalton Trans. 40 (2011) 10268–10277;
(d) D.Y. Du, L.K. Yan, Z.M. Su, S.L. Li, Y.Q. Lan, E.B. Wang, Coord. Chem. Rev. 257 (2013) 702–717.
[9] (a) C. Wang, T. Zhang, W.B. Lin, Chem. Rev. 112 (2012) 1084–1104;
(b) W. Zhang, R.G. Xiong, Chem. Rev. 112 (2012) 1163–1195;
(c) P.G. Lacroix, I. Malfant, J. Real, V. Rodriguez, Eur. J. Inorg. Chem. 2013 (2013) 615–627;
(d) D.F. Weng, Z.M. Wang, S. Gao, Chem. Soc. Rev. 40 (2011) 3157–3181;
(e) F. Riobé, N. Avarvari, Coord. Chem. Rev. 254 (2010) 1523–1533.
[10] C. Train, M. Gruselle, M. Verdaguer, Chem. Soc. Rev. 40 (2011) 3297–3312.
[11] (a) N. Berova, P.L. Polavarapu, K. Nakanishi, R.W. Woody, Comprehensive Chiroptical Spectroscopy: Instrumentation, Methodologies, and Theoretical Simulations, vol. 1, John Wiley & Sons, Inc., New Jersey, 2012;
(b) N. Berova, P.L. Polavarapu, K. Nakanishi, R.W. Woody, Comprehensive Chiroptical Spectroscopy: Applications in Stereochemical Analysis of Synthetic Compounds, Natural Products, and Biomolecules, vol. 2, John Wiley & Sons, Inc., New Jersey, 2012.
[12] J.P. Riehl, F.S. Richardson, Chem. Rev. 86 (1986) 1–16.
[13] (a) G. Holzwarth, E.C. Hsu, H.S. Mosher, T.R. Faulkner, A. Moscowitz, J. Am. Chem. Soc. 96 (1974) 251–252;
(b) L.D. Barron, M.P. Bogaard, A.D. Buckingham, J. Am. Chem. Soc. 95 (1973) 603–605.
[14] S. Abbate, E. Castiglioni, F. Gangemi, R. Gangemi, G. Longhi, Chirality 21 (2009) E242–E252.
[15] J. Hudecová, V. Profant, P. Novotná, V. Baumruk, M. Urbanová, P. Bouř, J. Chem. Theory Comput. 9 (2013) 3096–3108.
[16] (a) M. Ziegler, A. von Zelewsky, Coord. Chem. Rev. 177 (1998) 257–300;
(b) S. Kaizaki, in: N. Berova, P.L. Polavarapu, K. Nakanishi, R.W. Woody (Eds.), Comprehensive Chiroptical Spectroscopy: Applications in Stereochemical Analysis of Synthetic Compounds, Natural Products, and Biomolecules, vol. 2, John Wiley & Sons, Inc., New Jersey, 2012, pp. 451–471.
[17] (a) J. Autschbach, Coord. Chem. Rev. 251 (2007) 1796–1821;
(b) J. Autschbach, L. Nitsch-Velasquez, M. Rudolph, Top. Curr. Chem. 298 (2011) 1–98;
(c) J. Autschbach, N. in:, P.L. Berova, K. Polavarapu, R.W. Nakanishi, Woody, Comprehensive Chiroptical Spectroscopy: Instrumentation, Methodologies, and Theoretical Simulations, vol. 1, John Wiley & Sons, Inc., New Jersey, 2012, pp. 593–642.
[18] B.L. Guennic, W. Hieringer, A. Gorling, J. Autschbach, J. Phys. Chem. A. 109 (2005) 4836–4846.
[19] (a) J. Autschbach, F.E. Jorge, T. Ziegler, Inorg. Chem. 42 (2003) 2867–2877;
(b) C. Diedrich, S. Grimme, J. Phys. Chem. A 107 (2003) 2524–2539.
[20] (a) F.E. Jorge, J. Autschbach, T. Ziegler, J. Am. Chem. Soc. 127 (2005) 975–985;
(b) J. Fan, T. Ziegler, Inorg. Chem. 47 (2008) 4762–4773;
(c) J. Fan, M. Seth, J. Autschbach, T. Ziegler, Inorg. Chem. 47 (2008) 11656–11668;
(d) J. Fan, J. Autschbach, T. Ziegler, Inorg. Chem. 49 (2010) 1355–1362;
(e) J. Fan, T. Ziegler, Chirality 23 (2011) 155–166;
(f) Y. Wang, Y.K. Wang, J.M. Wang, Y. Liu, Y.T. Yang, J. Am. Chem. Soc. 131 (2009) 8839–8847.
[21] (a) T. Bark, A. von Zelewsky, D. Rappoport, M. Neuburger, S. Schaffner, J. Lacour, J. Jodry, Chem. Eur. J. 10 (2004) 4839–4845;
(b) P.W. Thulstrup, E. Larsen, Dalton Trans. 35 (2006) 1784–1789;
(c) F.J. Coughlin, K.D. Oyler, R.A. Pascal Jr., S. Bernhard, Inorg. Chem. 47 (2008) 974–979;
(d) T. Wu, X.P. Zhang, C.H. Li, P. Bouř, Y.Z. Li, X.Z. You, Chirality 24 (2012) 451–458.
[22] M. Jawiczuk, M. Goírecki, A. Suszczyníska, M. Karchier, J. Jazíwiníski, J. Frelek, Inorg. Chem. 52 (2013) 8250–8263.
[23] M. Enamullah, A.K.M. Royhan Uddin, G. Pescitelli, R. Berardozzi, G. Makhloufi, V. Vasylyeva, A. Chamayoud, C. Janiak, Dalton Trans. 43 (2014) 3313–3329.
[24] (a) S.G. Telfer, T.M. McLean, M.R. Waterland, Dalton Trans. 40 (2011) 3097–3108;
(b) P. Bouř, T.A. Keiderling, J. Am. Chem. Soc. 114 (1992) 9100–9105;
(c) J. Šebek, P. Bouř, J. Phys. Chem. A 112 (2008) 2920–2929.
[25] (a) X. Huang, B.H. Rickman, B. Borhan, N. Berova, K. Nakanishi, J. Am. Chem. Soc. 120 (1998) 6185–6186;
(b) V. Valderreya, G. Aragaya, P. Ballester, Coord. Chem. Rev. 258–259 (2014) 137–156.
[26] L. You, G. Pescitelli, E.V. Anslyn, L. Di Bari, J. Am. Chem. Soc. 134 (2012) 7117–7125.
[27] E.R. Kay, D.A. Leigh, F. Zerbetto, Angew. Chem., Int. Ed. 46 (2007) 72–191.
[28] J.W. Canary, S. Mortezaei, J. Liang, Coord. Chem. Rev. 254 (2010) 2249–2266.
[29] (a) S. Graule, M. Rudolph, N. Vanthuyne, J. Autschbach, C. Roussel, J. Crassous, R. Réau, J. Am. Chem. Soc. 131 (2009) 3183–3185;
(b) L. Norel, M. Rudolph, N. Vanthuyne, J.A.G. Williams, C. Lescop, C. Roussel, J. Autschbach, J. Crassous, R. Réau, Angew. Chem., Int. Ed. 49 (2010) 99–102;
(c) E. Anger, M. Rudolph, C. Shen, N. Vanthuyne, L. Toupet, C. Roussel, J. Autschbach, J. Crassous, R. Réau, J. Am. Chem. Soc. 133 (2011) 3800–3803;
(d) E. Anger, M. Srebro, N. Vanthuyne, L. Toupet, S. Rigaut, C. Roussel, J. Autschbach, J. Crassous, R. Réau, J. Am. Chem. Soc. 134 (2012) 15628–15631.
[30] (a) P.L. Polavarapu, J. Phys. Chem. A 109 (2005) 7013–7023;
(b) P.L. Polavarapu, Chem. Rec. 7 (2007) 125–136;
(c) J. Autschbach, Chirality 21 (2009) E116–E152.

[31] (a) G. Muller, Dalton Trans. 44 (2009) 9692–9707;
(b) R. Carr, N.H. Evans, D. Parker, Chem. Soc. Rev. 41 (2012) 7673–7687.
[32] K.E. Gunde, A. Credi, E. Jandrasics, A. von Zelewsky, F.S. Richardson, Inorg. Chem. 36 (1997) 426–434.
[33] K.D. Oyler, F.J. Coughlin, S. Bernhard, J. Am. Chem. Soc. 129 (2007) 210–217.
[34] (a) C. Schaffner-Hamann, A. von Zelewsky, A. Barbieri, F. Barigelletti, G. Muller, J.P. Riehl, A. Neels, J. Am. Chem. Soc. 126 (2004) 9339–9348;
(b) F.J. Coughlin, M.S. Westrol, K.D. Oyler, N. Byrne, C. Kraml, E. Zysman-Colman, M.S. Lowry, S. Bernhard, Inorg. Chem. 47 (2008) 2039–2048.
[35] (a) J.E. Field, G. Muller, J.P. Riehl, D. Venkataraman, J. Am. Chem. Soc. 125 (2003) 11808–11809;
(b) K. Nakamura, S. Furumi, M. Takeuchi, T. Shibuya, K. Tanaka, J. Am. Chem. Soc. 136 (2014) 5555–5558.
[36] C.S. Shen, E. Anger, M. Srebro, N. Vanthuyne, K.K. Deol, T.D. Jefferson Jr., G. Muller, J.A.G. Williams, L. Toupet, C. Roussel, J. Autschbach, R. Réau, J. Crassous, Chem. Sci. 5 (2014) 1915–1927.
[37] J.L. Lunkley, D. Shirotani, K. Yamanari, S. Kaizaki, G. Muller, J. Am. Chem. Soc. 130 (2008) 13814–13815.
[38] (a) J.L. Lunkley, D. Shirotani, K. Yamanari, S. Kaizaki, G. Muller, Inorg. Chem. 50 (2011) 12724–12732;
(b) D. Shirotani, H. Sato, K. Yamanari, S. Kaizaki, Dalton Trans. 41 (2012) 10557–10567.
[39] P.J. Stephens, F.J. Devlin, J.R. Cheeseman, VCD Spectroscopy for Organic Chemists, CRC Press, Boca Raton, FL, 2012.
[40] F.J. Devlin, P.J. Stephensa, P. Besse, Tetrahedron: Asymmetry 16 (2005) 1557–1566.
[41] (a) M.R. Oboodi, B.B. Lal, D.A. Young, T.B. Freedman, L.A. Nafie, J. Am. Chem. Soc. 107 (1985) 1547–1556;
(b) D.A. Young, E.D. Lipp, L.A. Nafie, J. Am. Chem. Soc. 107 (1985) 6205–6213;
(c) D.A. Young, T.B. Freedman, E.D. Lipp, L.A. Nafie, J. Am. Chem. Soc. 108 (1986) 7255–7263.
[42] Y. He, X. Cao, L.A. Nafie, T.B. Freedman, J. Am. Chem. Soc. 123 (2001) 11320–11321.
[43] (a) J.R. Cheeseman, M.J. Frisch, F.J. Devlin, P.J. Stephens, Chem. Phys. Lett. 252 (1996) 211–220;
(b) P.J. Stephens, J. Phys. Chem. 89 (1985) 748–752.
[44] (a) H. Sato, T. Taniguchi, K. Monde, S.I. Nishimura, A. Yamagishi, Chem. Lett. 35 (2006) 364–365;
(b) H. Sato, T. Taniguchi, A. Nakahashi, K. Monde, A. Yamagishi, Inorg. Chem. 46 (2007) 6755–6766;
(c) H. Sato, Y. Mori, Y. Fukuda, A. Yamagishi, Inorg. Chem. 48 (2009) 4353–4361.
[45] H. Mori, A. Yamagishi, H. Sato, J. Chem. Phys. 135 (2011) 084506.
[46] L.A. Nafie, J. Phys. Chem. A 108 (2004) 7222–7231.
[47] C. Johannessen, P.W. Thulstrup, Dalton Trans. 36 (2007) 1028–1033.
[48] S.R. Domingos, A. Huerta-Viga, L. Baij, S. Amirjalayer, D.A.E. Dunnebier, A.J.C. Walters, M. Finger, L.A. Nafie, B. de Bruin, W.J. Buma, S. Woutersen, J. Am. Chem. Soc. 136 (2014) 3530–3535.
[49] T.B. Freedman, X. Cao, D.A. Young, L.A. Nafie, J. Phys. Chem. A 106 (2002) 3560–3565.
[50] V.P. Nicu, J. Autschbach, E.J. Baerends, Phys. Chem. Chem. Phys. 11 (2009) 1526–1538.
[51] S. Lo Piano, S. Di Pietrob, L. Di Bari, Chem. Commun. 48 (2012) 11996–11998.
[52] (a) P. Schwerdtfeger, R. Bast, J. Am. Chem. Soc. 126 (2004) 1652–1653;
(b) F. De Montigny, R. Bast, A.S.P. Gomes, G. Pilet, N. Vanthuyne, C. Roussel, L. Guy, P. Schwerdtfeger, T. Saueh, J. Crassous, Phys. Chem. Chem. Phys. 12 (2010) 8792–8803.
[53] (a) P.R. Lassen, L. Guy, I. Karame, T. Roisnel, N. Vanthuyne, C. Roussel, X. Cao, R. Lombardi, J. Crassous, T.B. Freedman, L.A. Nafie, Inorg. Chem. 45 (2006) 10230–10239;
(b) F. De Montigny, L. Guy, G. Pilet, N. Vanthuyne, C. Roussel, R. Lombardi, T.B. Freedman, L.A. Nafie, J. Crassous, Chem. Commun. 46 (2009) 4841–4843;
(c) N. Saleh, S. Zrig, T. Roisnel, L. Guy, R. Bast, T. Saue, B. Darquie, J. Crassous, Phys. Chem. Chem. Phys. 15 (2013) 10952–10959.
[54] (a) G. Szilvágyi, Z. Majer, E. Vass, M. Hollósi, Chirality 23 (2011) 294–299;
(b) Z. Majer, G. Szilvágyi, L. Benedek, A. Csámpai, M. Hollósi, E. Vass, Eur. J. Inorg. Chem. 2013 (2013) 3020–3027.
[55] (a) T. Taniguchi, K. Monde, J. Am. Chem. Soc. 134 (2012) 3695–3698;
(b) T. Wu, X.Z. You, J. Phys. Chem. A 116 (2012) 8959–8964.
[56] G. Szilvágyi, B. Brém, G. Báti, L. Tölgyesi, M. Hollósi, E. Vass, Dalton Trans. 42 (2013) 13137–13144.
[57] A.C. Chamayou, S. Lüdeke, V. Brecht, T.B. Freedman, L.A. Nafie, C. Janiak, Inorg. Chem. 50 (2011) 11363–11374.
[58] C. Merten, K. Hiller, Y.J. Xu, Phys. Chem. Chem. Phys. 14 (2012) 12884–12891.
[59] C. Merten, Y.J. Xu, Dalton Trans. 42 (2013) 10572–10578.
[60] C. Merten, R. McDonald, Y.J. Xu, Inorg. Chem. 53 (2014) 3177–3182.
[61] C. Jahier, M.F. Coustou, M. Cantuel, N.D. McClenaghan, T. Buffeteau, D. Cavagnat, M. Carraro, S. Nlate, Eur. J. Inorg. Chem. 2011 (2011) 727–738.
[62] P.J. Stephens, F.J. Devlin, C. Villani, F. Gasparrini, S.L. Mortera, Inorg. Chim. Acta 361 (2008) 987–999.
[63] C. Merten, M. Amkreutz, A. Hartwig, J. Mol. Struct. 970 (2010) 101–105.
[64] H. Sato, D. Shirotani, K. Yamanari, S. Kaizaki, Inorg. Chem. 49 (2010) 356–358.
[65] S. Kaizaki, D. Shirotani, H. Sato, Phys. Chem. Chem. Phys. 15 (2013) 9513–9515.
[66] H. Sato, F. Sato, M. Taniguchi, A. Yamagishi, Dalton Trans. 41 (2012) 1709–1712.
[67] H. Sato, A. Yamagishi, Int. J. Mol. Sci. 14 (2013) 964–978.
[68] T. Wu, C.H. Li, Y.Z. Li, Z.G. Zhang, X.Z. You, Dalton Trans. 39 (2010) 3227–3232.
[69] T. Wu, X.P. Zhang, X.Z. You, Y.Z. Li, P. Bouř, ChemPlusChem 79 (2014) 698–707.
[70] T. Wu, C.H. Li, X.Z. You, Vib. Spectrosc. 63 (2012) 451–459.
[71] T. Wu, X.P. Zhang, X.Z. You, RSC Adv. 3 (2013) 26047–26051.
[72] D.W. Armstrong, F.A. Cotton, A.G. Petrovic, P.L. Polavarapu, M.M. Warnke, Inorg. Chem. 46 (2007) 1535–1537.
[73] E. Castiglioni, P. Biscarini, S. Abbate, Chirality 21 (2009) E28–E36.
[74] (a) G. Tian, G.S. Zhu, X.Y. Yang, Q.R. Fang, M. Xue, J.Y. Sun, Y. Wei, S.L. Qiu, Chem. Commun. 41 (2005) 1396–1398;
(b) Z.B. Han, J.W. Ji, H.Y. An, W. Zhang, G.X. Han, G.X. Zhang, L.G. Yang, Dalton Trans. 38 (2009) 9807–9811.
[75] (a) X.P. Zhang, T. Wu, J. Liu, J.C. Zhao, C.H. Li, X.Z. You, Chirality 25 (2013) 384–392;
(b) X.P. Zhang, T. Wu, J. Liu, J.X. Zhang, C.H. Li, X.Z. You, J. Mater. Chem. C 2 (2014) 184–194.
[76] S. Luber, M. Reiher, Chem. Phys. 346 (2008) 212–223.
[77] S. Luber, M. Reiher, ChemPhysChem 11 (2010) 1876–1887.
[78] C. Merten, H. Li, X. Lu, A. Hartwig, L.A. Nafie, J. Raman Spectrosc. 41 (2010) 1563–1565.
[79] C. Johannessen, L. Hecht, C. Merten, ChemPhysChem 12 (2011) 1419–1421.
[80] S. Yamamoto, P. Bouř, Angew. Chem. Int. Ed. 51 (2012) 1–5.
[81] (a) J.L. Zuo, X.Z. You, Chin. Sci. Bull. 46 (2001) 178–184;
(b) E. Cariati, M. Pizzotti, D. Roberto, F. Tessore, R. Renato Ugo, Coord. Chem. Rev. 250 (2006) 1210–1233;
(c) P.G. Lacroix, I. Malfant, J. Real, V. Rodriguez, Eur. J. Inorg. Chem. 2013 (2013) 615–627.
[82] X.L. Li, K. Chen, Y. Liu, Z.X. Wang, T.W. Wang, J.L. Zuo, Y.Z. Li, Y. Wang, J.S. Zhu, J.M. Liu, Y. Song, X.Z. You, Angew. Chem. Int. Ed. 46 (2007) 6820–6823.
[83] D.P. Li, C.H. Li, J. Wang, L.C. Kang, T. Wu, Y.Z. Li, X.Z. You, Eur. J. Inorg. Chem. 2009 (2009) 4844–4849.
[84] J. Liu, X.P. Zhang, T. Wu, B.B. Ma, T.W. Wang, C.H. Li, Y.Z. Li, X.Z. You, Inorg. Chem. 51 (2012) 8649–8651.
[85] Y. Sui, D.P. Li, C.H. Li, X.H. Zhou, T. Wu, X.Z. You, Inorg. Chem. 49 (2010) 1286–1288.
[86] H.T. Zhang, Y.Z. Li, T.W. Wang, E.N. Nfor, H.Q. Wang, X.Z. You, Eur. J. Inorg. Chem. 2006 (2006) 3532–3536.
[87] Q. Ye, Y.Z. Tang, X.S. Wang, R.G. Xiong, Dalton Trans. 34 (2005) 1570–1573.
[88] X.Q. Liang, D.P. Li, X.H. Zhou, Y. Sui, Y.Z. Li, J.L. Zuo, X.Z. You, Cryst. Growth Des. 9 (2009) 4872–4883.
[89] X.Q. Liang, J.T. Jia, T. Wu, D.P. Li, L. Liu, Tsolmon, G.S. Zhu, CrystEngComm 12 (2010) 3499–3501.
[90] W. Zhang, H.Y. Ye, R.G. Xiong, Coord. Chem. Rev. 253 (2009) 2980–2997.
[91] C.N.R. Rao, A.K. Cheetham, A. Thirumurugan, J. Phys. Condens. Matter 20 (2008) 083202.
[92] T.J. Boyle, S.D. Bunge, P.G. Clem, J. Richardson, J.T. Dawley, L.A.M. Ottley, M.A. Rodriguez, B.A. Tuttle, G.R. Avilucea, R.G. Tissot, Inorg. Chem. 44 (2005) 1588–1600.
[93] S. Horiuchi, Y. Tokura, Nat. Mater. 7 (2008) 357–366.
[94] (a) V. Krstic, S. Roth, M. Burghard, K. Kern, G.L.J.A. Rikken, J. Chem. Phys. 117 (2002) 11315–11319;
(b) V. Krstic, G.L.J.A. Rikken, Chem. Phys. Lett. 364 (2002) 51–56.
[95] (a) J.T. Chalker, S.L. Sondhi, Phys. Rev. B: Condens. Matter 59 (1999) 4999–5002;
(b) A. Kleiner, Phys. Rev. B: Condens. Matter 67 (2003) 155311–155315;
(c) R. Roy, C. Kallin, Phys. Rev. B: Condens. Matter 77 (2008) 174513–174517.
[96] (a) N. Avarvari, J.D. Wallis, J. Mater. Chem. 19 (2009) 4061–4076;
(b) F. Pointillart, S. Golhen, O. Cador, L. Ouahab, Dalton Trans. 42 (2013) 1949–1960;
(c) J.I. Yamada, TTF Chemistry: Fundamentals and Applications of Tetrathiafulvalene, Springer-Verlag, Berlin and Heidelberg, 2004;
(d) R. Wang, L.C. Kang, J. Xiong, X.W. Dou, X.Y. Chen, J.L. Zuo, X.Z. You, Dalton Trans. 40 (2011) 919–926.
[97] E. Coronado, R. Galan-Mascaros Jose, J. Gomez-Garcia Carlos, A. Murcia-Martinez, E. Canadell, Inorg. Chem. 43 (2004) 8072–8077.
[98] C. Rethore, N. Avarvari, E. Canadell, P. Auban-Senzier, M. Fourmigue, J. Am. Chem. Soc. 127 (2005) 5748–5749.
[99] A.M. Madalan, C. Réthoré, N. Avarvari, Inorg. Chim. Acta 360 (2007) 233–240.
[100] J. Lieffrig, O. Jeannin, P. Auban-Senzier, M Fourmigué, Inorg. Chem. 51 (2012) 7144–7152.
[101] F. Pop, S. Laroussi, T. Cauchy, C.J. Gomez-Garcia, J.D. Wallis, N. Avarvari, Chirality 25 (2013) 466–474.
[102] (a) M. Clemente-Leon, E. Coronado, C. Marti-Gastaldoza, F.M. Romeroab, Chem. Soc. Rev. 40 (2011) 473–497;
(b) G. Rogez, C. Massobrio, P. Rabu, M. Drillon, Chem. Soc. Rev. 40 (2011) 1031–1058.
[103] (a) E. Coronado, J.R. Galan-Mascaros, C.J. Gomez-Garcia, V. Laukhin, Nature 408 (2000) 447–449;
(b) S. Ohkoshi, H. Tokoro, T. Matsuda, H. Takahashi, H. Irie, H. Hashimoto, Angew. Chem. Int. Ed. 46 (2007) 3238–3241;
(c) E. Pardo, C. Train, H.B. Liu, L. Chamoreau, B. Dkhil, K. Boubekeur, F. Lloret, K. Nakatani, H. Tokoro, S. Ohkoshi, M. Verdaguer, Angew. Chem. Int. Ed. 51 (2012) 1–6.
[104] (a) L.D. Barron, Nat. Mater. 7 (2008) 691–692;
(b) C. Train, R. Gheorghe, V. Krstic, L.M. Chamoreau, N.S. Ovanesyan, G. Rikken, M. Gruselle, M. Verdaguer, Nat. Mater. 7 (2008) 729–734.

[105] (a) G. Wagniere, A. Meier, Chem. Phys. Lett. 93 (1982) 78–81;
(b) L.D. Barron, J. Vrbancich, Mol. Phys. 51 (1984) 715–730.
[106] (a) G.L.J.A. Rikken, E. Raupach, Phys. Rev. E: Stat. Phys. Plasmas Fluids Relat. Interdisciplin. Top. 58 (1998) 5081–5084;
(b) G.L.J.A. Rikken, E. Raupach, Nature 390 (1997) 493–494.
[107] P. Kleindienst, G.H. Wagniere, Chem. Phys. Lett. 288 (1998) 89–97.
[108] (a) M. Mannini, F. Pineider, P. Sainctavit, C. Danieli, E. Otero, C. Sciancalepore, A.M. Talarico, M.A. Arrio, A. Cornia, D. Gatteschi, R. Sessoli, Nat. Mater. 8 (2009) 194–197;
(b) M. Mannini, F. Pineider, P. Sainctavit, L. Joly, A. Fraile-Rodriguez, M.A. Arrio, C. Cartier dit Moulin, W. Wernsdorfer, A. Cornia, D. Gatteschi, R. Sessoli, Adv. Mater. 21 (2009) 167–171.
[109] W.X. Zhang, R. Ishikawa, B. Breedlovea, M. Yamashita, RSC Adv. 3 (2013) 3772–3798.
[110] P. Gerbier, N. Domingo, J. Gomez-Segura, D. Ruiz-Molina, D.B. Amabilino, J. Tejada, B.E. Williamson, J. Veciana, J. Mater. Chem. 14 (2004) 2455–2460.
[111] E. Pardo, C. Train, R. Lescouezec, Y. Journaux, J. Pasan, C. Ruiz-Perez, F.S. Delgado, R. Ruiz-Garcia, F. Lloret, C. Paulsen, Chem. Commun. 46 (2010) 2322–2324.
[112] L. Sorace, C. Benelli, D. Gatteschi, Chem. Soc. Rev. 40 (2011) 3092–3104.
[113] (a) R. Sessoli, A.K. Powell, Coord. Chem. Rev. 253 (2009) 2328–2341;
(b) D.N. Woodruff, R.E.P. Winpenny, R.A. Layfield, Chem. Rev. 113 (2013) 5110–5148;
(c) P. Zhang, Y.N. Guo, J.K. Tang, Coord. Chem. Rev. 257 (2013) 1728–1763.
[114] D.P. Li, T.W. Wang, C.H. Li, D.S. Liu, Y.Z. Li, X.Z. You, Chem. Commun. 46 (2010) 2929–2931.
[115] J. Ru, F. Gao, T. Wu, M.X. Yao, Y.Z. Li, J.L. Zuo, Dalton Trans. 43 (2014) 933–936.
[116] K.M. Ok, E.O. Chi, P.S. Halasyamani, Chem. Soc. Rev. 35 (2006) 710–717.
[117] K. Ikeda, S. Ohkoshi, K. Hashimoto, J. Appl. Phys. 93 (2003) 1371–1375.
[118] T. Nuida, T. Matsuda, H. Tokoro, S. Sakurai, K. Hashimoto, S. Ohkoshi, J. Am. Chem. Soc. 127 (2005) 11604–11605.
[119] C. Train, T. Nuida, R. Gheorghe, M. Gruselle, S.I. Ohkoshi, J. Am. Chem. Soc. 131 (2009) 16838–16843.
[120] S.I. Ohkoshi, S. Takano, K. Imoto, M. Yoshikiyo, A. Namai, H. Tokoro, Nat. Photonics 8 (2014) 65–71.
[121] (a) N.A. Spaldin, M. Fiebig, Science 309 (2005) 391–392;
(b) W. Eerenstein, N.D. Mathur, J.F. Scott, Nature 442 (2006) 759–765.
[122] C.F. Wang, Z.G. Gu, X.M. Liu, J.L. Zuo, X.Z. You, Inorg. Chem. 47 (2008) 7957–7959.
[123] T. Sasaki, I. Hisaki, T. Miyano, N. Tohnai, K. Morimoto, H. Sato, S. Tsuzuki, M. Miyata, Nat. Commun. 4 (2013) 1787.
[124] D.T. McLaughlin, T.P.T. Nguyen, L. Mengnjo, C. Bian, Y.H. Leung, E. Goodfellow, P. Ramrup, S. Woo, L.A. Cuccia, Cryst. Growth Des. 14 (2014) 1067–1076.
[125] (a) C. He, Y.G. Zhao, D. Guo, Z.H. Lin, C.Y. Duan, Eur. J. Inorg. Chem. 2007 (2007) 3451–3463;
(b) X.D. Zheng, T.B. Lu, CrystEngComm 12 (2010) 324–336.
[126] (a) Y.S. Xia, Y.L. Zhou, Z.Y. Tang, Nanoscale 3 (2011) 1374–1382;
(b) A. Ben-Moshe, B.M. Maoz, A.O. Govorov, G. Markovich, Chem. Soc. Rev. 42 (2013) 7028–7041.
[127] T.R. Cook, V. Vajpayee, M.H. Lee, P.J. Stang, K.W. Chi, Acc. Chem. Res. 46 (2013) 2464–2474.